

BSPE99862-12486-7

2020. 12

# 황해-북동중국해 대륙붕 퇴적물의 기원지(S2S) 정량화 연구

[www.kiost.ac.kr](http://www.kiost.ac.kr)

Quantification of Sediment Source-to-sink (S2S) in the Yellow and  
northern East China Seas

# 제 출 문

한국해양과학기술원장 귀하

본 보고서를 “황해-북동중국해 대륙붕 퇴적물 기원지(S2S) 정량화 연구 (Quantification of Sediment Source-to-sink (S2S) in the Yellow and northern East China Seas)”과제의 최종보고서로 제출합니다.

2020.12.

총괄연구책임자 : 임 동 일

참 여 연 구 원 : 김지훈, 이준호  
정도현, 정희수  
하현주

## 보고서 초록

과제고유 번호	BSPE99862-1 2486-7	해당단계 연구기간	2020.02.01- 2020.12.31	단계 구분	
연구사업명	중사업명				
	세부사업명				
연구과제명	대과제명	신진,중견연구자의 연구기반 구축 및 창의적 아이디어 지원			
	세부과제명	황해-북동중국해 대륙붕 퇴적물 기원지(S2S) 정량화 연구			
연구책임자	임동일	해당단계 참여연구원수	총 : 6 명 내부: 6 명 외부:    명	해당단계 연구비	정부: 100,000천원 기업:       천원 계 : 100,000천원
		총연구기간 참여연구원수	총 : 6 명 내부: 6 명 외부:    명	총 연구비	정부: 100,000천원 기업:       천원 계 : 100,000천원
연구기관명 및 소속부서명	한국해양과학기술원 남해연구소		참여기업명		
국제공동연구					
위탁연구					
요 약				보고서 면수	82
<p>○ 연구 배경: 지난 30년간 황해-북동중국해 퇴적물의 기원과 이동 등의 퇴적환경을 이해하기 위해 많은 연구가 이루어져 왔으나, 최근 S2S(source-to-sink)에 대한 기존 연구들의 상반된 결과와 해석 그리고 객관적인 자료 부족 등 여러 문제점이 제기되어 왔음. 더욱이 대부분의 기존 연구가 정성적 분석(qualitative analysis)에 머물러 있어, 기원지별 퇴적물의 기여도 및 퇴적량에 대한 정량적 평가(quantification)는 미해결 난제로 남아 있음. 또한, 냉수대와 전선역 등의 환경-생태학적 역할 규명 그리고 육상-대기 오염물질 유입-이동-확산, 실트 경계 설정 등의 해양과학기술 현안 대응에 대한 국가적 기반역량 강화를 위해서도 S2S의 정량적 연구가 필요함</p> <p>○ 연구 목표 : 황해-북동중국해 퇴적물의 기원지별 정량적 판별을 위한 지화학적 추적자 모델을 개발·구축하고, 시·공간적 정량화 분포도 작성 및 변동 해석</p> <p>○ 주요 결과: 1) 황해-북동중국해 표층(400 정점) 및 코어(14 정점_200 시료) 퇴적물의 주성분(Al, Fe, Mg 등) 및 희토류(rare earth elements) 원소 성분 특성을 분석함(기존 해양시료 활용), 2) 기원지를 판별할 수 있는 지화학적 추적자(Al-Fe-Mg-REEs)를 도출함, 3) Al-Mg 회귀 분석 정량화 모델과 REE 분별화 지수 정량화 모델을 개발·구축함, 4) 황해-북동중국해 전 해역의 퇴적물 기원지별 기여도 정량화 및 시·공간적 분포도를 작성함, 5) 황해-북동중국해 퇴적물 기원-운반-퇴적(S2S) 기작과 퇴적량을 정량적으로 해석함, 6) 연구결과 논문 게재(Marine Geology, 2020, 230, 106345, Contiental Shelf Research, 2021, in press)</p>					
색인어 (각 5개 이상)	한 글	황해-북동중국해, 지화학적 프락시, 퇴적물 기원지, 기여도 정량화			
	영 어	Yellow-northern East China Seas, geochemical proxy, sediment source-to-sink, quantification			

# 요 약 문

## I. 제 목

황해-북동중국해 퇴적물 기원지(S2S) 정량화 연구 (Quantification of sediment source-to-sink (S2S) in the Yellow and northern East China Seas)

## II. 연구개발의 필요성

- 황해-북동중국해에서 퇴적물 기원, 이동, 확산, 퇴적(source-to-sink, S2S) 등의 퇴적환경을 이해하기 위한 다양하고 많은 연구가 이루어져 왔으나, 황해-북동중국해 전 해역을 커버하는 해양과학적 자료 부재 그리고 기존 연구들 사이의 상반된 결과와 해석 등 여러 문제점이 제기됨
- 특히 황해-북동중국해의 퇴적물 기원지에 관한 대부분의 연구가 정성적 분석(qualitative analysis)에 머물러 있어, 기원지별 퇴적물의 기여도 및 퇴적량에 대한 정량적 평가(quantification)는 해양(지질)과학적 미해결 난제로 남아 있음
- 따라서 S2S에 대한 신뢰성 있는 객관적 자료와 해석을 위해서는 황해-동중국해 전 해역에 대한 시료 확보와 일관성 있는 유의미한 분석 자료 도출과 함께 기원지의 정성적(qualitative analysis) 분석에서 정량적(quantification) 분석 단계로의 해양과학기술 고도화 및 퇴적물의 기원-이동-확산-퇴적과정에 대한 표준화 모델 정립 필요
- 또한, 퇴적물 기원지의 정량적 분석 연구를 통해 황해 냉수대와 전선역 등의 환경-생태학적 역할 그리고 육상·대기 오염물질 유입-이동-확산 등의 해양과학기술 현안 대응에 대한 국가적 기반역량 강화 필요

## III. 연구개발의 내용 및 범위

- 황해-북동중국해 퇴적물의 기원지별 정량적 기여도 산정을 위한 지화학적 정량화 모델 개발
  - 퇴적물 기원지별(한국과 중국 강 기원) 지화학 성분의 “end-member” 도출
  - 퇴적물 기원지별 기여도의 정량적 평가를 위한 지화학적 모델 구축
- 황해-동중국해 전 해역 퇴적물 기원지 정량화 및 시·공간적 분포도 작성과 변동 해석
  - 황해-북동중국해 전 해역 퇴적물 기원지 판별과 정량화의 시·공간적 변동 특성
  - 퇴적물 이동-퇴적과정(S2S) 종합 해석 (기후변화, 전선역-냉수대 역할, 쿠로시오 변동 등)
- 황해-동중국해에서의 퇴적물 기원지 판별과 이동에 관한 연구를 기존의 정성적(qualitative analysis) 분석에서 정량적(quantification) 평가 단계로의 해양과학기술 고도화
- 해양시료도서관 해양시료자원의 재활용을 통한 황해-북동중국해 전 해역 퇴적물 분석·활용

## IV. 연구개발 결과

- 본 연구를 위해 황해-북동중국해의 연안과 대륙붕 전 해역을 포함하는 약 400정점에서 표층 및 코어 퇴적물(표층 400 정점, 코어 퇴적물 14 정점의 약 200점 부시료) 시료의 주성분

(major elements) 및 희토류 (rare earth elements, REEs) 성분 특성을 분석함. 특정 시료에 대해서는 퇴적물 입자의 크기별(size fractionation), 결합형태별(labile and residual fractionation) 원소 성분 특성을 분석함

- 분석 결과, Fe, Mg와 REEs 성분 등은 기원지별(한국 및 중국 강) 정량화 판별을 위한 유용한 지화학적 추적자로 판명됨. 특히, Fe와 Mg 함량의 경우 같은 퇴적물 입자 크기에서 한국 강 퇴적물과 비교하여 중국 강 퇴적물에서 높고, REEs의 경우 중국 강 퇴적물에서 middle-REE가 상대적으로 높은 특징을 보임
- 이러한 지화학적 추적자를 활용하여 황해-북동중국해에서 한국과 중국 강 퇴적물의 기여도를 정량적으로 판별하기 위한 새로운 “Al-Mg 회귀직선 모델”과 “REE fractionation 지수 모델”을 개발·구축함.
- 개발된 황해-북동중국해 전 해역 퇴적물 시료에 대한 기원지별 기여도를 정량화하고, 시·공간적 분포도 작성함. 특징적으로 약 124°E 기준으로 한국과 중국의 강 퇴적물이 약 50%씩 혼합된 것으로 평가됨. 또한, 중국 강 퇴적물의 기여도는 황해중앙니질대(CYSM) 퇴적물에서 55-80% 그리고 황해남동니질대(SEYSM, 흑산니질대) 퇴적물에서 10-40% 범위로, 퇴적물 입자 크기에 따라 변화함.
- 기원지별 기여도는 퇴적시기에 따라서도 크게 변화하며, 특히 중국 기원 퇴적물은 7천년전(7 kyr BP) 이후부터 황해-북동중국해에 퇴적되기 시작한 것으로 해석되며, 약 3-4천년전(3-4 kyr BP)의 전지구적 아빙하기(cold event) 동안 쿠로시오 해류의 약화에 따라 중국 기원 퇴적물의 공급이 일시적으로 중단된 것으로 나타남
- 황해-북동중국해 퇴적물 기원지의 시·공간적 분포 특성과 퇴적물 이동은 기후변화, 쿠로시오 해류의 변동과 세기, 전선대, 냉수대, 지형 등의 복합적 요인에 의해 조절되는 것으로 해석됨

## V. 연구결과 활용계획

- 황해-동중국해에서 발생하는 제반 해양환경(특히 해양오염), 해양생태자원, 해양경계획정 문제 등에 대처하기 위한 해양과학기술적 핵심 자료로 활용
- 해양과학적 현안 연구중 하나인 퇴적물 기원지의 정량적 판별 문제를 해결함으로써 한반도 주변 해양환경-생태계에 대한 지식기반 확립
- 기존 해양시료자원의 재사용을 통한 창의적 연구 활성화 촉진
- 퇴적물의 기원지를 판별하는 효과적/경제적 분석 기술 확보
  - 오염 물질의 기원과 확산 추적/예측하고 제어하는 기술 개발에 응용 가능

**주요 핵심어** : 황해-북동중국해, 지화학적 프락시, 퇴적물 기원지, 기여도 정량화, 해양시료자원

# S U M M A R Y

## **I. Title**

Quantification of sediment source to-sink (S2S) in the Yellow and northern East China Seas

## **II. Necessity of the research**

- The Yellow and northern East China Seas (YECSs) has been extensively studied for the understanding of dispersal patterns and limits of sediments from neighboring countries including China and Korea. Although various sedimentological-geochemical-mineralogical approaches have been tried to solve the issues such as sediment origins, budgets, sediment accumulation rates, the published results are not enough for understanding them and sometimes even controversial. In this respect, the sediment provenance in the YECSs has long been a subject of interest, but its quantification is still inconclusive.
- With the oceanographic and sedimentological complexity, sediment source identification of the YECS sediments has been a challenge; in particular, information on the source-to-sink transport pathways within the YECS basin and how the sediment supply rate from those sources have changed over time is still limited. Thus, there remains a clear need to continue refining and scrutinizing quantitative examinations on the YECS sediment fingerprints for improving the robustness of source discrimination.
- This study provides a better understanding of the present- and paleo-depositional systems of the YECSs, successfully capturing land-ocean interactions and paleoenvironmental changes in the northwestern Pacific margin during the Holocene. And also, this research is necessary to strengthen the ocean science and technology capability to respond to national maritime policy issues such as environmental pollution problem, maritime boundary delimitation (e.g., silt line) and marine management in the YECSs.

## **III. Research scope and contents**

- Development of new estimation model for quantifying the sediment source-to-sink (S2S) of the YECS sediments
  - Suggestion of new geochemical proxies for discriminating the sediment sources (Korean and Chinese river sediments)
  - Sediment S2S quantification model development using these geochemical proxies
- Application of quantification model to the YECS sediments and interpretation of spatio-temporal variation in quantitative source apportionments
  - Contemporary spatial sediment source-to-sink quantification
  - Temporal variations of sediment S2S quantification over the last 20 kyr
  - Oceanographic-climatic forcings on the spatio-temporal variations sediment source
- Technological advances in the YECS sediment source-to-sink analysis from qualitative to quantitative estimation

- A creative research on reuse of the sediment sample resource of LIMS (Library of Marine Samples)

#### IV. Research Results

- We performed an element compositional (major and REEs) analysis on all surface (400 samples) and core (14 cores, 200 subsamples) sediment samples from the YECS for more robust and accurate data acquisition and interpretation. To better constrain geochemical links of YECS deposits to source rocks and provide more robust insights on their origins, further, elemental compositions of some sediments were granulometrically (silt and clay populations) and chemically (labile and residual phases) partitioned.
- Our results revealed that some major elements (i.g, Fe and Mg) and REEs are unequivocal tracers for provenance identification of the YECS sediments. Although both the Korea river (KR) and Chinese river (CR) source groups have similar grain sizes, Fe and Mg are more enriched in the CR sediments, and also the REE fractionation patterns are significantly different between them.
- In this study, we proposed new sediment source proxy models (i.e., Al–Mg regression model and REE–fractionation index model) that reflects innate characteristics of their fractionation distribution patterns and provides a reasonable and practical estimation for quantifying sediment source apportionments in the YECSs.
- The spatio–temporal variations in quantitative source apportionment of the CR sediments based on these models showed abrupt decline in the CR contribution at around 124°E, which indicates a boundary of the CR sediment transportation to the eastern part of the Yellow Sea. Our quantitative source estimates clearly depict a considerable supply of the CR sediments (~50%) to the southwestern Korean coastal region (SEYSM deposit), and the KR sediments (30–40%) to the CYSM deposit, which accounts for a good balance between the sediment supply and budget of the shelf deposit.
- On the basis of the REE–source index model, meanwhile, proportional contributions of CR sediments to the central (CYSM) and southeastern Yellow Sea mud (SEYSM) deposits were estimated to be 55–80% and 10–40%, respectively.
- Further, the observed variations in proportions between Huanghe–, Changjiang– and Korean river–derived sediments over the last 15 kyr – notably an abrupt increase of CR contribution since ~7 ka, followed by a sudden drop at ~3–4 ka – exhibit a good correspondence with other mineralogical proxy records.
- These temporal provenance changes witnessed robust palaeoenvironmental signals which fit to major climatic and oceanographic events linked with sea–level, intensity of the Kuroshio Current inflow and the East Asian monsoon. This study improves understanding of what pathways and sinks exist within the YECS basin, and how rates of sediment supply from adjacent rivers have changed over time.

## V. Application of the research results

- Used as core data for national policy establishment to respond to marine science issues such as marine environments, marine ecological resources, and maritime boundary delimitation occurring in the YECSs
- Establishing a knowledge base for marine environments and ecosystems around the Korean seas by solving the problem of quantitative apportionment of sediment sources, which is one of the challenges of current marine science research
- Applicable to the development of technology to track and predict the occurrence and spread of pollutants
- Promotion of creative research through reuse of LIMS's marine sample resources

**Keywords:** Yellow-northern East China Sea, geochemical proxy, sediment source-to-sink (S2S), quantification model



# 목 차

제 1 장 서 론 .....	1
제 2 장 Al-Mg을 활용한 퇴적물의 기원지별 기여도 정량화 및 시공간적 분포 특성 .....	5
제 1 절 연구배경 .....	6
제 2 절 분석방법 .....	9
제 3 절 Al-Mg 선형 회귀분석을 활용한 기원지 정량화 모델 .....	10
제 4 절 기원지별 정량화의 시-공간적 분포 .....	17
제 5 절 현재 퇴적물 기원지 변동 원인과 기작 .....	21
제 6 절 요약 .....	26
제 3 장 희토류(REEs) 성분을 활용한 기원지 정량화 .....	28
제 1 절 연구배경 .....	29
제 2 절 분석방법 .....	32
제 3 절 입자별, 결합 형태별 희토류 성분의 fractionation 특성 .....	33
제 4 절 희토류 성분을 활용한 퇴적물 기원지 정량화 모델 .....	38
제 5 절 요약 .....	44
제 4 장 결 론 .....	46
제 5 장 참고문헌 .....	49
제 6 장 부 록 .....	62

# C O N T E N T S

<b>Chapter 1. Introduction</b> .....	<b>1</b>
<b>Chapter 2. Quantification reconstruction of Holocene sediment source variations using Al-Mg linear regression</b> .....	<b>5</b>
1. Research background .....	6
2. Materials and methods .....	9
3. Al-Mg regression analysis for sediment fingerprinting and source apportionment .....	10
4. Contemporary spatial sediment source-to-sink quantification .....	17
5. Oceanographic-climatic forcings on the Holocene sediment source variations ....	21
6. Conclusions .....	26
<b>Chapter 3. REE fractionation and sediment source quantification</b> .....	<b>28</b>
1. Research background .....	29
2. Materials and methods .....	32
3. Fractionation distribution characteristics of REE partitioning .....	33
4. New source discrimination model using REE fractionation distribution .....	38
5. Conclusions .....	44
<b>Chapter 4. Summary</b> .....	<b>46</b>
<b>Chapter 5. References</b> .....	<b>49</b>
<b>Chapter 6. Appendix</b> .....	<b>62</b>

# Chapter 1



## Introduction

Marine sediments provide an invaluable key for unlocking a hidden history of Earth's climate system as well as a window into future climate projections. The sediment deposits of the Yellow and East China Seas (YECSs) include contributions of massive river inputs from the Korean Peninsula and mainland China (~15 billion tons per year; 10% of the world's river sediment discharge to the ocean). These sediment deposits have been considered as an ideal benchmark region for studying the complex interactions between the land–ocean processes of Earth's climate system. A sound understanding of the different terrestrial components recorded in marine sediments, as well as the origins of these terrestrial components, is essential for ongoing global climate research. The sediments of the YECSs vary widely with respect to their multiple riverine sources, and provide a fundamental basis for investigating not only the marine environment ecosystem and its resources, but also the delimitation of the Yellow Sea's maritime boundaries. This study aims to develop a novel sediment fingerprinting technique for a more precise quantitative estimation of sediment source proportions in the YECSs.

The YECSs, one of the well-known epicontinental marginal seas in the western Pacific, occupies the broad continental shelf between the Korean peninsula and the Chinese mainland, and receives a vast amount of sediment, which comes mainly from the Huanghe of China. The sea has several small and large source rivers entering from the neighboring countries (Korea and China), with their various spectrums of basin rock composition, as well as complex coastal and shelf current systems affected by the locations of river mouths (Guan, 1994; Yang et al., 2003a and references therein; Li et al., 2006; Yang et al., 2009). Characteristically, on the shelf, there are several isolated mud depositions that were deposited and transported by large seasonal and spatial variations of coastal and shelf currents coupled with the Yellow Sea Warm Current (Zhu and Chang, 2000; Bian et al., 2013). Until now, much effort has been expended to discriminate sediment origin (e.g., Korean Han, Keum and Yeongsan Rivers or Chinese Huanghe and

Changjiang) in the coastal and shelf mud depositions of the sea, especially by employing geochemical techniques (e.g., Cho et al., 1999; Yang et al., 2003a; Yang and Youn, 2007; Jung et al., 2012; Lim et al., 2013), because such sediment provenance information might improve our understanding of the present complex depositional system and enable assessment of paleoceanographic reconstructions (e.g., evolution of the Kuroshio and coastal currents) (e.g., Lim et al., 2007; Wang et al., 2014). Considering the comparatively small sediment load of Korean rivers, it has been presumed that the sea is overwhelmingly covered by sediments supplied by the Chinese rivers. However, several studies have suggested that the sediments of the sea (especially the central and southeastern coastal areas of the Yellow Sea) consist of a mixture of Korean (KR) and Chinese river (CR) sediments (e.g., Yang et al., 2003a; Lim et al., 2006, 2007, 2013 and references therein; Bian et al., 2013). This suggestion has created a new paradigm in study of the sediment provenance of the Yellow Sea and highlights its importance. With the oceanographic and sedimentological complexity, accordingly, sediment source identification of the YECS deposits has been a challenge; in particular, information on the source-to-sink transport pathways within the YECS basin and how the sediment supply rate from those sources have changed over time is still limited. It may be primarily due to a lack of reasonable and practicable estimation methods. Thus, there remains a clear need to continue refining and scrutinizing quantitative examinations on the YECS sediment fingerprints for improving the robustness of source discrimination. By developing a new sediment source-to-sink fingerprinting technique, we aim to enhance the level of sediment provenance studies that have always been qualitative to semi-quantitative methods and to upgrade the capability of Marine Science and Technology.


The main objectives of this study is as follows: 1) Development of new estimation model for quantifying the YECS sediment source-to-sink (S2S): suggestion of new geochemical proxies for discriminating the sediment sources (Korean and Chinese river sediments) and S2S quantification model development

using these geochemical proxies. 2) Application of quantification model to the YECS sediments and spatio-temporal variations in quantitative source apportionments: contemporary spatial sediment source-to-sink quantification, temporal variations of sediment S2S quantification over the last 20 kyr, and oceanographic-climatic forcings on the spatio-temporal variations sediment source. In this study, as a result, we suggested new models (Al-Mg regression model and REE-source index model) for quantifying sediment source in the YECSs. These quantification estimations well define spatiotemporal sediment source-to-sink dynamics in the sea. The results provide significant insights on dispersal systems of riverine sediments in the sea.

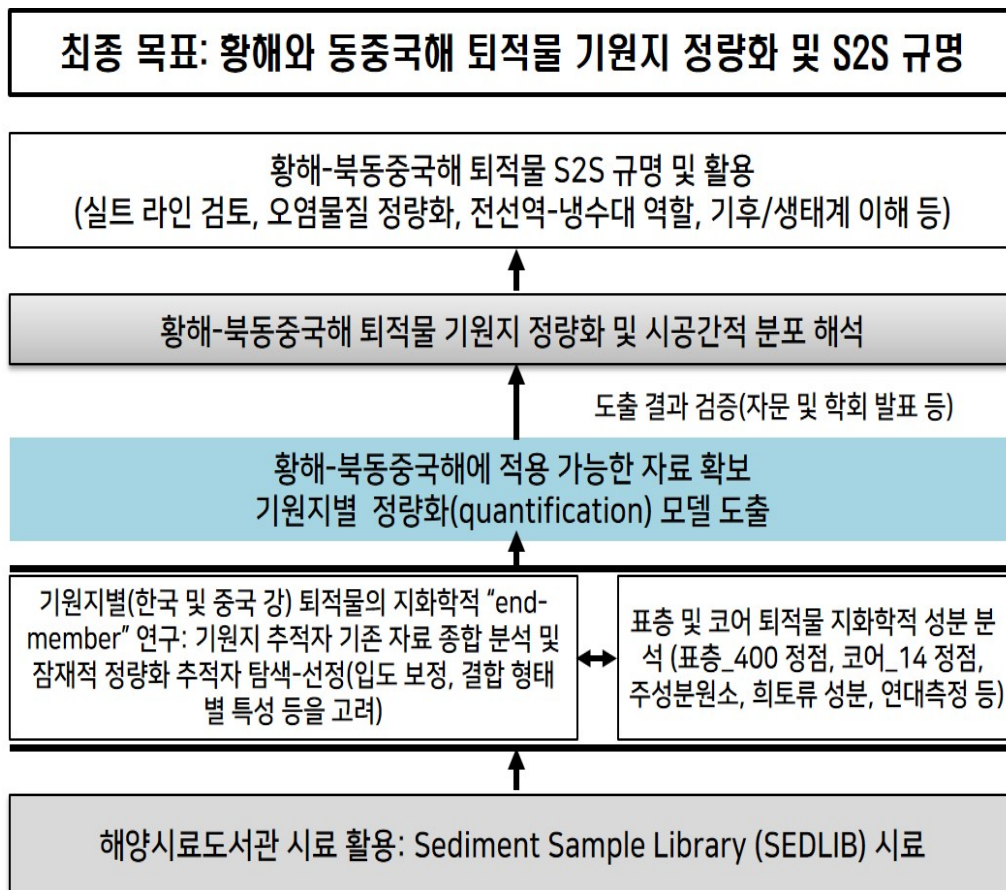


**Figure 1.** Tactics for sediment source quantification in the YECSs.

# Chapter 2



Quantification reconstruction of  
Holocene sediment source variations  
using Al-Mg linear regression

## 1. Research background

The East Asian marginal seas form a transition between the world's largest continent and its largest ocean, representing major sediment repositories of information on an interaction between the two realms, with a wide variance in their responses to climatic and environmental changes. The Yellow and northern East China Seas (YECSs, Fig. 1a), a representative of East Asian marginal seas, are characterized by broad continental shelves and huge terrigenous sediment inputs from the largest and most turbid rivers on Earth (e.g., Huanghe, Changjiang, and several small Korean rivers) (Milliman and Meade, 1983). These terrigenous sediments form several unique muddy depositional patches and belts on the shelves that are basically determined by diverse riverine sediment sources with various spectrums of bedrock compositions, old deltaic sediment shifts, complicated transport processes associated with strong tidal rearrangement, and intricate coastal-shelf current patterns that include historical variations of the Kuroshio (Yang et al., 2003; Lim et al., 2007, 2015a; Bian et al., 2013; Wang et al., 2014). This complexity in the formation of the shelf muddy deposits makes the YECSs an ideal natural laboratory for the study of sediment source-to-sink dynamics and land–sea interactions during the late Quaternary (e.g., Gao and Collins, 2014; Li et al., 2014a, 2016a; Yang et al., 2014b; Wang et al., 2019).

In view of this, the sediment source-to-sink and related depositional processes in the YECSs have been widely studied over the past decades, and several plausible explanations have been proposed. However, there is still an ongoing and controversial debate about the source discrimination and dispersal pattern of the sediments (Yang et al., 2003; Lim et al., 2006; Bian et al., 2013; Wang et al., 2014). For example, notwithstanding the notion that the Yellow Sea sediments are mostly derived from Chinese rivers (CR) (e.g., Milliman et al., 1985; Ren and Shi, 1986; Alexander et al., 1991; Park and Khim, 1992), there have been little evidence of the CR sediment transports to the eastern portion of the Yellow Sea.



In fact, there is growing evidence for a greater contribution of Korean river (KR)-sourced sediments to the eastern and even central portions of the sea (e.g., Lee and Chu, 2001; Chough et al., 2002; Li et al., 2014b; Lim et al., 2015a; Rao et al. 2015; Wang et al., 2014). Further, recent findings reveal more complicated source origins, as can be seen from the central region of the Yellow Sea (e.g., Zhao et al., 1990, 1997; Wei et al., 2003; Lim et al., 2007; Li et al., 2014b; Wang et al., 2014) and as far as the Korean coastal zone (Lim et al., 2007, 2013; Cho et al., 2015; Um et al., 2015). With such oceanographic and sedimentological complexity, provenance identification of the YECS sediments has been a challenge; in particular, information on the source-to-sink transport pathways within the YECS basin and how the sediment supply rate from those sources have changed over time are still limited. Thus, there remains a clear need to continue refining and scrutinizing quantitative examinations on the YECS sediment fingerprints for improving the robustness of source discrimination.

Despite a wide range of application of sediment source tracers – mainly geochemical properties (e.g., alkaline-earth elements, REEs and Nd-Sr isotopes), existing work using these fingerprinting in the YECS sediments has tended to produce rather equivocal signals (Yang et al., 2003a). Recently, Lim et al. (2006, 2015b) recognized a significant potential of some alkaline earth elements including Mg and Fe as elemental fingerprints in identifying different sources of fine-grained YECS sediments. By implementing the preliminary work of Lim et al. (2006), we propose an alternative approach of the YECS sediment source quantification based on the advanced Al-Mg regression model, with the aim to increase its application effectiveness. To support this overview, we explored spatiotemporal variations of the YECS sediment source apportionments by applying this tracing approach to historic sedimentary deposits as well as contemporary spatial sediments over the region. The present study provides a broader understanding of the present- and paleo-depositional systems of the YECSs, successfully capturing land–ocean

interactions and paleoenvironmental changes in the northwestern Pacific margin during the Holocene.

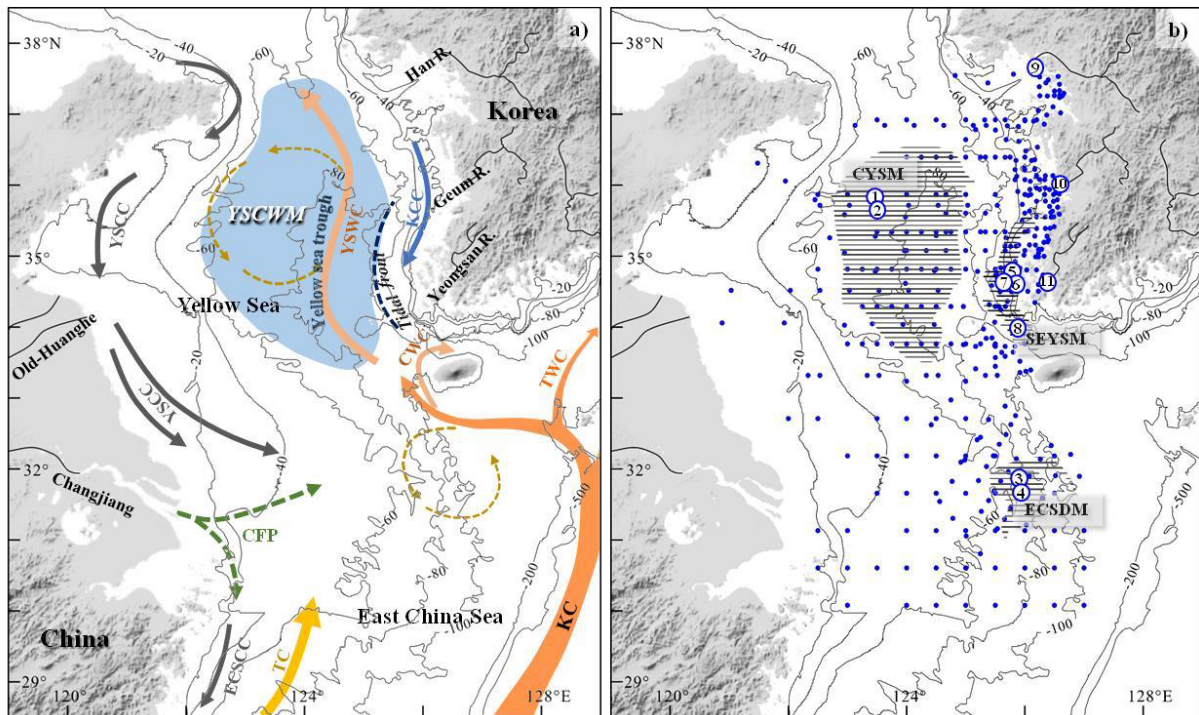


**Figure 1.** (a) A map showing the study area including the current system. KC: Kuroshio Current, TC: Taiwan Warm Current, ECSCC: East China Sea Coastal Current, TWC: Tsushima Warm Current, CWC: Cheju Warm Current, YSWC: Yellow Sea Warm Currents, YSCC: Yellow Sea Coastal Currents, CFP: Changjiang Freshwater Plume, KCC: Korean Coastal Current, YSCWM: Yellow Sea Cold Water Mass (after Hu, 1984; Chen, 2009; Liu et al., 2007; Yu et al., 2016). (b) Sampling sites of the surface (n = 399), and core sediment samples (n = 14) for the study. Hatched areas indicate the mud deposits. CYSM: Central Yellow Sea Mud, SEYSM: Southeastern Yellow Sea Mud (or Huksan Mud Belt, HMB), ECSDM: East China Sea Distal Mud (or Southwestern Cheju Island Mud, SWCIM). Dots: surface sediments, Numbers: sediment cores E61, E65, E310, E410, Y21, E619, YSDP103, YSDP102, NY9203 and YGC06, YC11 and YGC1, and YGC11 and YGC13.

## 2. Materials and methods

For this study, a total of 399 surface sediments from the coastal and shelf zones of the YECSs, and 14 sediment cores from the several mud patches (Central Yellow Sea Mud, CYSM: 2 cores, Southeastern Yellow Sea Mud, SEYSM: 4 cores, East China Sea Distal Mud, ECSDM: 2 cores, and Korean coastal zone: 6 cores) have been investigated (Fig. 1b). For an improved demonstration of land–ocean interactions and paleoenvironmental changes in the YECS regime, we applied a new fingerprinting technique to two deep-drilled cores, YSDP102 (~60 m in core length) and 103 (~35 m in core length), from the SEYSM (or Hunksan Mud Belt) patch (KIGAM, 1996).

Grain-size analyses for some surface sediments ( $n = 179$ ) were carried out using a standard dry-sieving technique for the sand fraction ( $> 63\mu\text{m}$ ), and the pipette method for the mud fraction ( $< 63\mu\text{m}$ ) after the removal of organic matters and carbonates.  $\text{Al}_2\text{O}_3$ , and  $\text{MgO}$  contents of all surface and core sediments together with standard reference material (MAG-1) were analyzed using an inductively coupled plasma atomic emission spectroscopy (ICP-AES) after a sequential pretreatment and acidic digestion (e.g., Lim et al., 2013). An accuracy of the analytical method was monitored by repeated measures ( $n = 58$ ) of the standard reference material together with a batch of sediment samples. The results showed that relative deviations between measured and known values were generally less than 2% ( $\text{Al}_2\text{O}_3 = 16.14\% \pm 0.20$ ,  $\text{MgO} = 3.01\% \pm 0.04$ ), indicating satisfactory recoveries. The bulk and chemical fractionation data of  $\text{Al}_2\text{O}_3$ ,  $\text{Fe}_2\text{O}_3$  and  $\text{MgO}$  contents for riverine sediments in this study are obtained from Lim et al. (2013, 2015b). Some outliers in the bulk compositional data of the riverine sediments are statistically removed. A dataset including grain size, carbon isotopic ratio ( $\delta^{13}\text{C}_{\text{org}}$ ), and oxygen index (OI) of Rock-Eval pyrolysis for the deep-drilled core YSDP102 and 103 sediments was obtained from KIGAM (1996).

Age model of deep-drilled core YSDP103 was constructed on the basis of

sedimentation rates reported by Park et al. (2000); sedimentation rates of the upper (0–18.2 m) and lower (18.6–32.4 m) sections of the core are 5.4 mm/yr and 2.4 mm/yr, respectively, which are quite comparable with those of Kong et al. (2006). Especially, two sections of the core are separated by a thin gravelly sand layer, suggesting a significant time gap or hiatus between them (Park et al., 2000; Kong et al., 2006; Chang and Ha, 2015; Lee et al., 2015). Ages of YSDP102 sediments were established based on a well-constructed chronostratigraphic framework for the SEYSM deposition; several stratigraphic studies, together with accelerator mass spectrometer  $^{14}\text{C}$  age data, also revealed that the YSDP102 deposit was accumulated during 7.0–3.5 ka (e.g., Park et al., 2000; Lee et al., 2014), with a sedimentation rate of 14.9 mm/yr. Meanwhile, age models of two short cores (E619 and YS21) collected near the YSDP102 coring site were reconstructed on the basis of an averaged sedimentation rate (3.9 mm/yr, Park et al., 2000) measured by using total  $^{210}\text{Pb}$  activities of the cores in this area.

### **3. Al-Mg regression analysis for sediment fingerprinting and source apportionment**

We performed an elemental compositional analysis on all YECS sediment samples for more robust and accurate data acquisition and interpretation, in an attempt to improve sensitivity of the fingerprint method established by the pioneering work of Lim et al. (2006).  $\text{Al}_2\text{O}_3$  and  $\text{MgO}$  contents in the YECS surface and core sediments ranged from 6.20% to 21.11% and 0.18% to 3.29%, respectively, which correspond well with variations in the mean grain-size distributions (Fig. 2), showing that sediment grain size is a primary factor affecting spatial and vertical distributions of these elements in the YECSs.

In several studies (i.e., Lim et al., 2006, 2013, 2015a), Fe and Mg have been regarded as unequivocal tracers for provenance identification of the YECS sediments. Indeed, plots of elements versus conservative Al in our study display

distinctive linear regression trends, along with different slopes for both the KR and CR sediment sources (Fig. 3a).

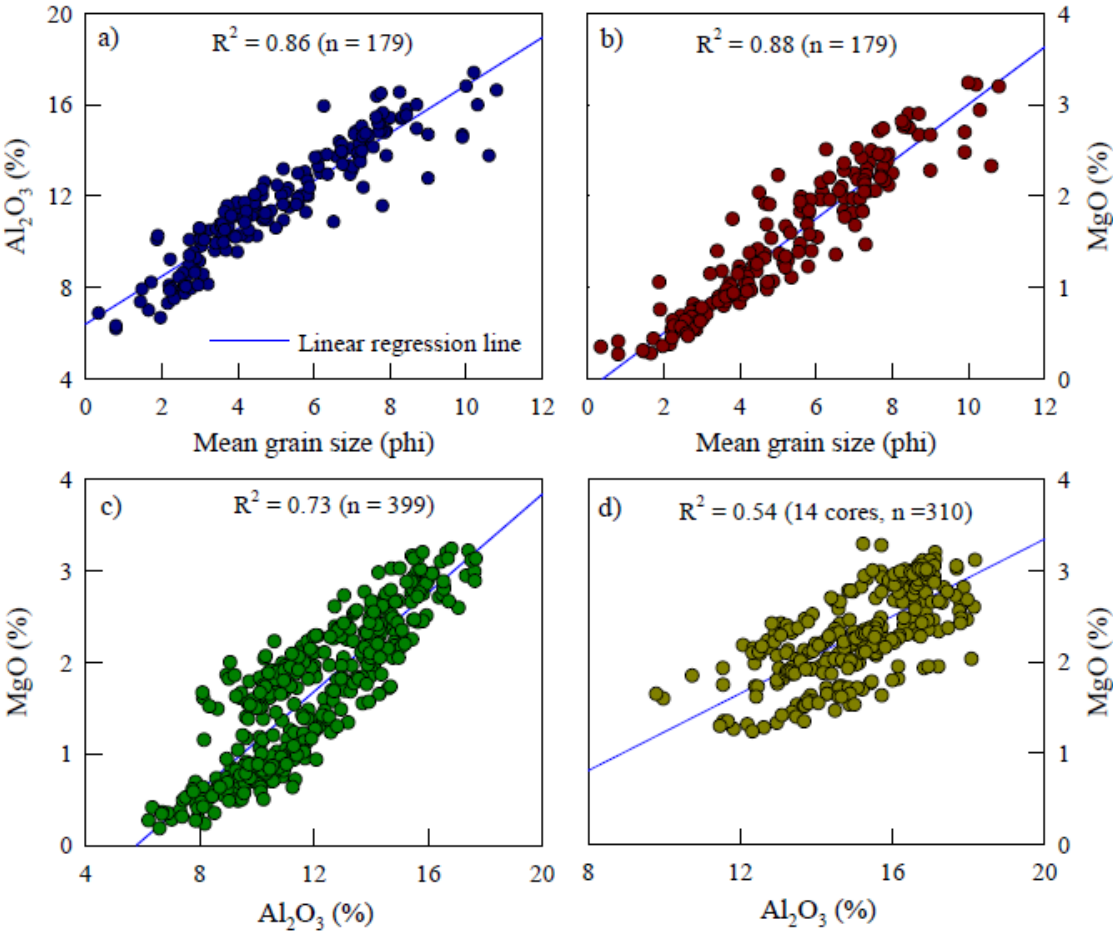


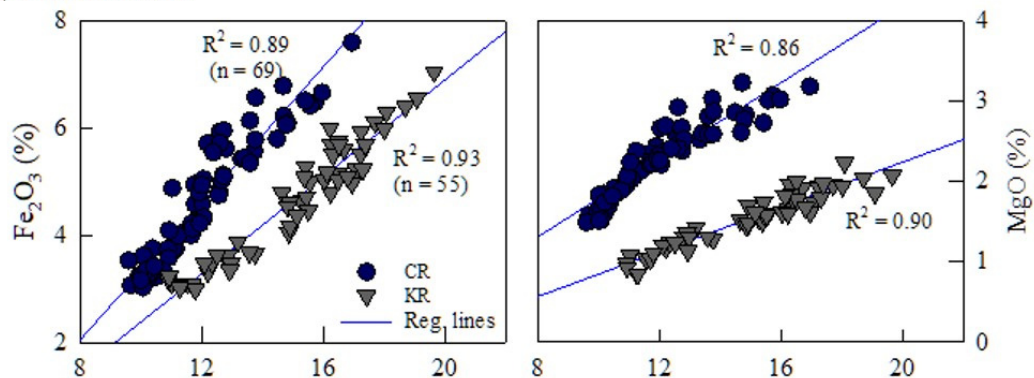
**Figure 2.** Bivariate plots of mean grain size, Al<sub>2</sub>O<sub>3</sub>, and MgO contents in (a–c) the surface sediments, and (d) the core sediments from the YECSs.

This geochemical disparity is also obvious in the grain-size (silt and clay fractions) and chemically partitioned (labile and detrital fractions) elements (Figs. 3b, c, and d), revealing that although both the KR and CR source groups have similar grain sizes, Fe and Mg are more enriched in the CR sediments. This geochemical dissimilarity between these riverine sediments might reflect inherited signatures of their source rocks; the bedrocks in Korea are dominated by Precambrian granite and gneiss and in China by complex basin rock compositions (i.e., Paleozoic carbonate rock, acidic metamorphic rocks, Quaternary clastic sediments, and loess deposits). Lim et al. (2015a) recently revealed that CR sediments can be of weathering products from relatively more mafic rocks (i.e., abundant ferromagnesian minerals and plagioclase feldspar minerals), which can be generally considered as granodiorite that would result in relatively high Fe, Mg, Ca, V, and Ni contents, and more radiogenic  $^{143}\text{Nd}/^{144}\text{Nd}$  ratios. In contrast, KR sediments are mostly derived from silicic granites, characterized by relatively higher quartz and potassium feldspar contents, tend to represent lower Fe and Mg and higher K.

Despite the fact that the source rock origin is one of crucial factors controlling chemical compositions of river sediments, there are secondary important processes, such as silicate weathering and geo- and physico-chemical alterations in river sediments (Nesbitt et al., 1980 and references therein; Babechuk et al., 2014; Dinis et al., 2017). Nevertheless, studies on chemical index of alteration (CIA) and Al/Na values – within a limited range of grain size (i.e., silt or clay size fractions) in the detrital fraction – showed that difference in the degrees of silicate weathering between the KR and CR sediments is not large, except for the clay-dominated fraction of the Huanghe sediments with its slightly lower intensity (Yang et al., 2004; Lim et al., 2015a). This supports the notion that such compositional dissimilarity, particularly in Fe and Mg contents may be stem from different source rock types (Yang et al., 2003; Lim et al., 2014, 2015a), by which

a provenance characterization of the shelf sediments can be achieved.

**a) Bulk sediments**



**b) Silt and clay fraction : total concentration**

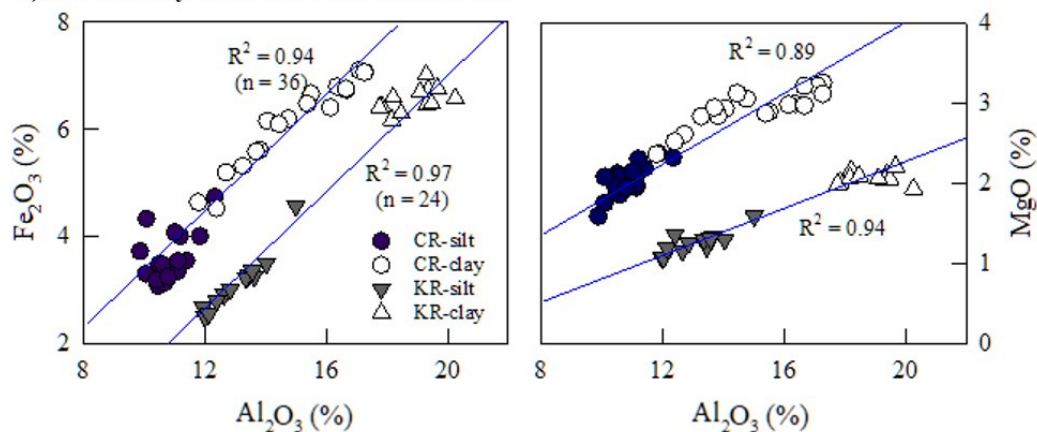


**Figure 3.** Al-Fe-Mg discriminant plots for Korean (KRs) and Chinese river (CRs) sediments: (a) total contents of bulk sediments, and (b) total, (c) labile (1 M hydrochloric acid-leachable phase), and (d) detrital (1 M hydrochloric acid-insoluble phase) phases of silt-dominated (60–20  $\mu\text{m}$ ) and clay-dominated (< 20  $\mu\text{m}$ ) fractions. Note a distinct compositional disparity between KR and CR sediments in grain-size and chemically partitioned elements (excluding Fe contents in labile fraction); given that both the KR and CR source groups have similar grain sizes, Mg are more enriched in the CR sediments. Data are taken from Lim et al. (2015a).

Unlike Mg, meanwhile, the labile fractions of Fe used failed to discriminate between the two river sediments (Fig. 3c), possibly due to secondary addition and amorphous Fe-hydroxides formed in the water column, in contrast to the differentiation provided by the detrital fraction. This casts doubt on the reliability of Fe as a tracer of river sources. Thus, the Al-Mg discrimination plot produces a more reasonable and robust provenance discrimination of YECS sediments. The alkaline earth elements (Mg, Ba, and Sr) has also been proposed as a potential proxy of sandy-sediment provenance in the YECSs (Kim et al., 1999).

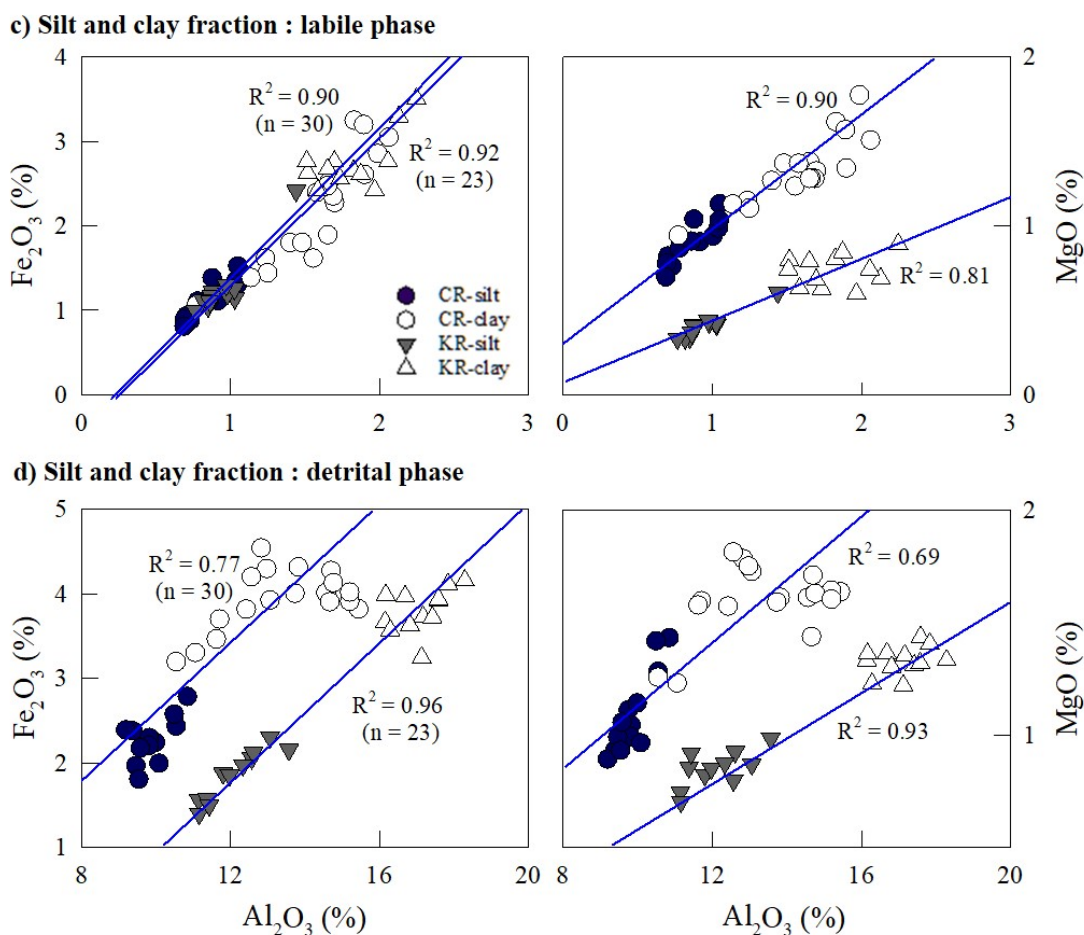


**Figure 3.** c) and d) (continued)



In the Al-Mg discrimination plot (Fig. 4), most of the surface and core sediment samples are scattered between the KR and CR sources, implying that they are a mixture of the two sources. To quantify source contributions of these sediments, we constructed an evaluation method using the different Al-Mg linear regression equations between both river source groups. The relative source contributions of each sample can be calculated from perpendicular distances between the location of a sediment sample and each of the linear regression lines (Fig. 4a). For this analysis, notably, the value of the  $(x, y)$  coordinate of the intersection point of the two regression lines was transformed to the origin  $(0, 0)$ , as the two lines were not parallel (Fig. 4a, see Lim et al., 2006 for more details); additionally, the Al and Mg contents of all sediment samples were also corrected using the transformed origin (Fig. 4b). This correction involves the normalization of bulk contents to account for differences of grain size in sediment geochemistry, which would enable more unequivocal sediment source discrimination in the YECSs (Lim et al., 2006). In the unlikely event that the intersection point of two linear lines with different slopes is not at the origin  $(0, 0)$ , for example, a simple calculation of the Mg/Al ratio may lead to a misinterpretation; specifically, the two river sediments is likely to be assigned the same source origin, with the same ratio value, by assuming that the best-fit linear regression line passes through the origin.

The method presented here provides a reasonable and practicable estimation for quantifying sediment provenance apportionment. For this, a normalization of bulk elemental contents to various sediment textures should be applied, especially for continental shelf sediments with uniquely different end-member sources.

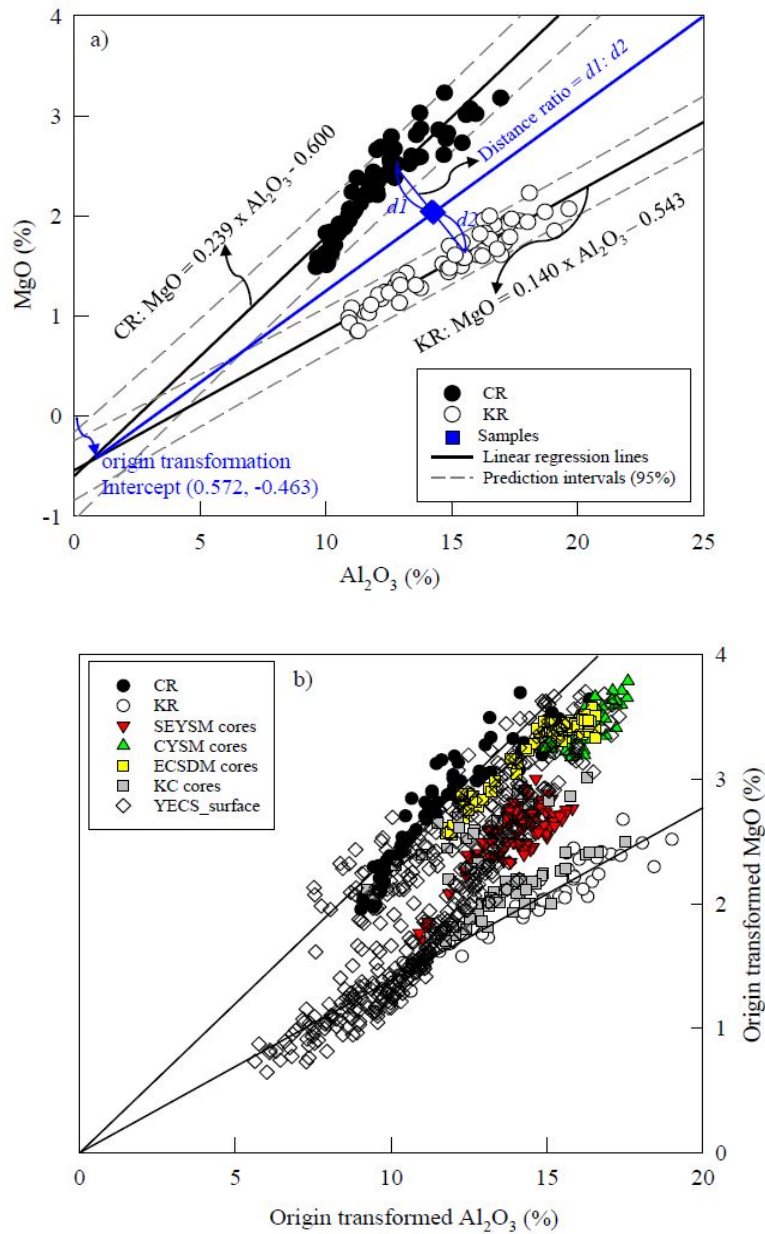


**Figure 4.** (a) Al-Mg linear regression model for quantitative sediment source discrimination of the Korean rivers (KRs) and Chinese rivers (CRs). For Al-normalization, in this study, the intersection point of the two regression lines of KR and CR sediments is used as the origin (0, 0). (b) Origin-transformed Al-Mg discriminant diagram for all sediment samples from the YECSs. Note that most of the surface and core sediment samples are scattered between the KR and CR sources, implying that they are a mixture of the two river sediments.

#### 4. Contemporary spatial sediment source-to-sink quantification

In this section, we examine whether the Al-Mg regression model-based sediment fingerprinting can provide robust constraints on source apportionments of sediments from the complex YECS catchment. The results over the entire YECS area reveal an unambiguous spatial distinction between the KR and CR attributions (Fig. 5). Overall, the northern East China Sea (ECS) shelf sediments, including the ECSDM (or Southwestern Cheju Island mud, SWCIM, Fig. 1a) are dominated by the CR sediments (>80% of the contribution) from the old-Huanghe delta, carried by the southward Yellow Sea Coastal Current (YSCC) and the Changjiang Freshwater Plume (CFP), and finally being trapped within a cyclonic upwelling gyre (Hu and Li, 1993; Xiang et al., 2006; Youn and Kim, 2011; Dou et al., 2015 and references therein). Of particular note is an abrupt decline in the CR contributions around 124°E (Figs. 5 and 6), indicating that the CR sediments do not reach the eastern part of the Yellow Sea blocked by this boundary, despite its massive supply (>10% of the world's fluvial sediment discharge, Hay, 1998).

A closer look on the aforementioned boundary shows a narrow zone (124–125°E) along the ~70-m depth contour of the Yellow Sea trough. This zone is characterized by an admixture of the KR and CR sources; the two sources appear to show a sudden drag as they pass across their ~60% contribution zone (Fig. 5). This notion gains support from an abrupt decrease in sediment accumulation rates from > 5 mm/yr to < 1 mm/yr (Lim et al., 2007; Qiao et al., 2017), which roughly overlaps with the center of the Yellow Sea Cold Water Mass (YSCWM, < 10°C, Yang et al., 2014a; Zhu et al., 2018), the deepest part of the Yellow Sea (Fig. 1a). One possible but still speculative explanation for this mixing zone could be overall stable condition of the YSCWM, which would prevent direct dispersal of the CR-sourced suspended matters from the coastal zone to the eastern Yellow Sea, thus acting as a “barrier” (e.g., Naimie et al., 2001; Wang et al., 2014; Li et al., 2019); the YSCWM developed in this area, together with a cyclonic eddy, is

of primary importance as it traps finer particles, resulting in the CYSM deposition.

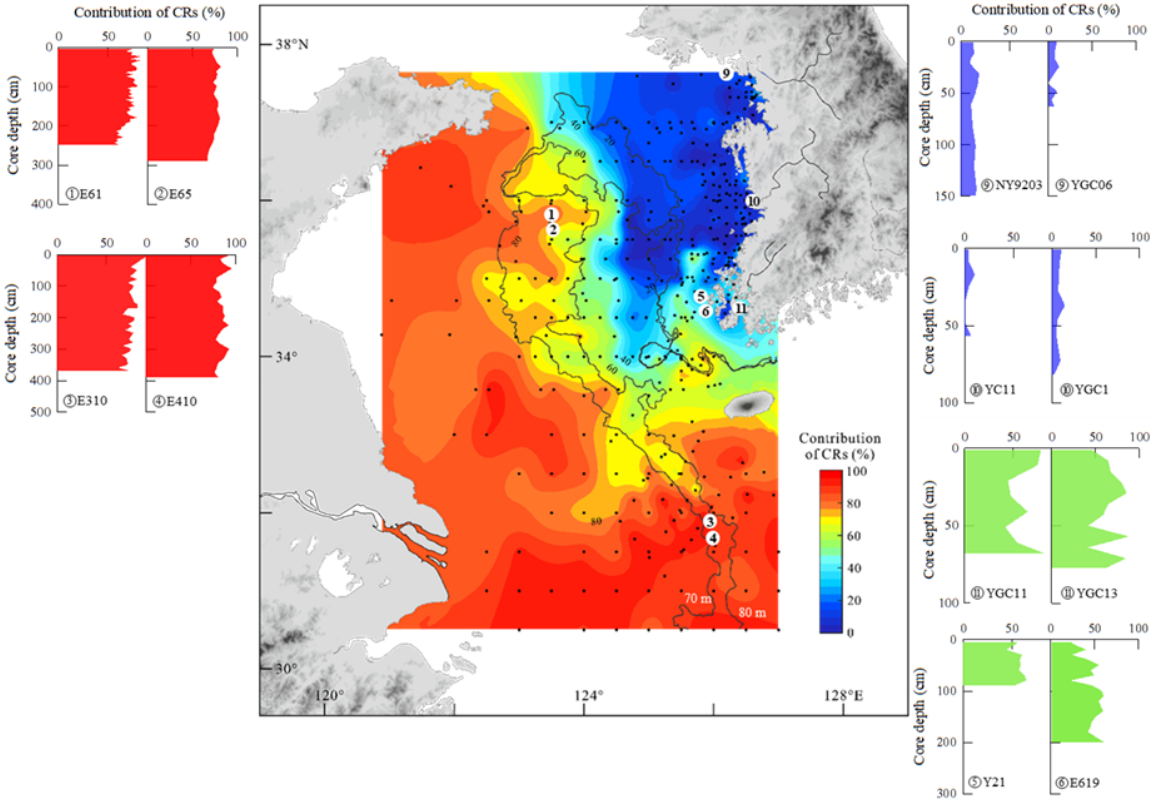


**Figure 5.** Spatio-temporal variations in quantitative source apportionments of the CR sediments in the YECSs. Note the abrupt decline in the CR contribution at around 124°E, which indicates a boundary of the CR sediments transportations to the eastern part of the Yellow Sea. Numbers represent the sediment cores.

That is, the YSCWM has a unique role to trap suspended sediment under the thermocline due to weakening tidal current and residual current there (Li et al., 2016a, Li et al., 2019). Additionally, a strong tidal front along the southwestern Korean coasts (Fig. 1a) would also restrict the KR-sourced (i.e., Geum and Youngsan rivers) sediments to be dispersed to the western Yellow Sea by surpassing the mixing zone (Lie, 1989; Lee and Chu, 2001; Ren et al., 2014). Given that the YSCC has a primary control over the CR sediment distributions over the YECS regime, this boundary, with two opposite water currents (the southward YSCC and the northward Yellow Sea Warm Current, YSWC), represents the weakest tidal-current and cyclonic eddy zone in the YSCWM (Shi et al., 2003; Hickox et al., 2000; Dong et al., 2011; Wang et al., 2014 and references therein). It is here that the CYSM deposit, with diverse sediment sources (Huanghe, Changjiang, and other small rivers, Zhao et al., 1990, 1997; Shi et al., 2003; Wei et al., 2003; Li et al., 2014b; Wang et al., 2014), can be developed. Another issue is the CR sediment supplies and contributions to the Korean coastal mud deposits, which has been an ongoing debate until recently (e.g., Lim et al., 2007, 2015b). In this regard, the predomination of the CR source in the Southeastern Yellow Sea Mud (SEYSM) deposit along the southwestern Korean coasts, with its sharp contrast to the adjacent region, is noteworthy (Fig. 5). Our estimates clearly depict a considerable supply of the CR sediments (~50%) to the southwestern Korean coastal region. This gains further support from the sediment cores of major mud depocenters in the Yellow Sea and Korean coastal regions; the CR contribution of the SEYSM core sediments was lower than that of the CYSM and ECSDM cores but was much higher than that of the Korean coastal cores (Fig. 5).

On the basis of total volume ( $1.03 \times 10^{11} \text{ m}^3$ , Lee et al., 2015) and dry bulk density (0.7–1.2  $\text{g/cm}^3$ ; mean: 1.0  $\text{g/cm}^3$ , Lee, 2015) of the SEYSM sediments, the total amount of sediments accumulated in the deposit over the last 7 kyrs (Lim et al., 2007) is estimated to be approximately  $1.47 \times 10^7 \text{ ton/yr}$ .

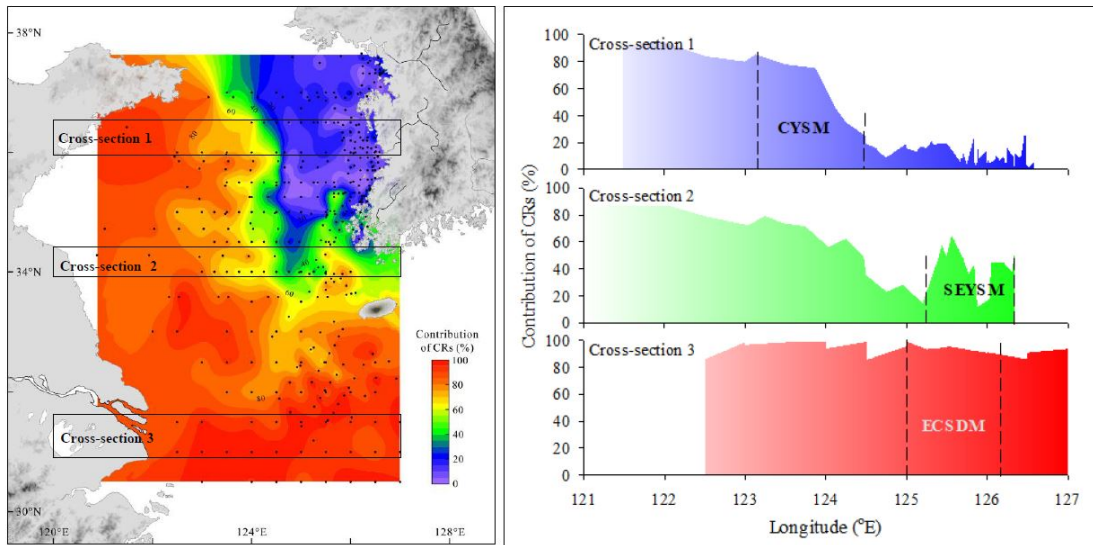


**Figure 6.** Cross-sectional distributions of the CR source contribution in the middle (cross-section1) and southern part (cross-section 2) of the Yellow Sea, and the northern East China Sea (cross-section 3).

However, given that sediment supply from the Geum and Yeongsan rivers of the Korea to the SEYSM deposit is a maximal rate of  $1.22 \times 10^7$  ton/yr if at least half of the riverine materials escape from the estuary and coastal zone (Lim et al., 2007) the actual sediment contribution of these rivers to the SEYSM would be only approximately  $6 \times 10^6$  ton/yr, which cannot account for the entire deposit. This means that additional sediment supplies to the SEYSM deposit another half of the total budget ( $\sim 8.7 \times 10^6$  ton/yr) needs to be further explained. Notably, the additional sediment supply can be drawn from quantitative estimates of the CR sediment contribution to the Korean coastal mud deposit; the CR sediment contribution to the SEYSM is estimated to be  $\sim 50\%$  on average (Fig. 5,  $\sim 7.4 \times 10^6$  ton/yr), which, in fact, compensates for the gap in the total sediment budget. Also, it has been suggested that fine-grained sediments from the old-Huanghe delta and/or the Changjiang are delivered to the northern ECS; at a later time, some of these sediments were reworked and transported to the inner shelf of Korea by the YSWC (Lim et al., 2007; Dou et al., 2015). Indeed, this notion is evidenced by

the tongue-shaped distribution (Fig. 5), in which the CR sediment accumulation decreases gradually from the southern (~60%) to the northern part (~30%) of the deposit. Considering all of the above, our results account for a good balance between the sediment supply and budget of the SEYSM deposit, which has been a subject of debate in studies of the Yellow Sea depositional system since the mid-2000s.

## **5. Oceanographic-climatic forcings on the Holocene sediment source variations**

Holocene sedimentation in the YECSs is epitomized by peculiar shelf muddy deposits (i.e., CYSM, SEYSM, and ECSDM, Fig. 1b), which are strongly connected to regional ocean circulation dynamics, including the Kuroshio (e.g., Dong et al., 2011; Hu et al., 2014; Gao et al., 2015; Zeng et al., 2015; Li et al., 2016a, b) and East Asian monsoon system (e.g., Wang et al., 2006; Wang and Yang, 2013; Kim and Lim, 2014; Li et al., 2014a; Lim et al., 2015a; Wang et al., 2019). In particular, the multi-sourced SEYSM deposit represents an essential sedimentary archive for temporal dynamics of the overall sediment delivery system, including a sediment source-to-sink flux in the YECSs in relation to the land–ocean–climate interactions during the Holocene. In this context, we quantitatively reconstructed sediment source variations of the SEYSM deposit over the last 15 kyr on the basis of our improved Al-Mg regression analysis (Fig. 7). To facilitate our interpretation along these lines, we also compared our results with the carbonate mineral proxy record of Hu et al. (2014) i.e., Huanghe-sourced calcite and Changjiang-sourced dolomite source variations in the ECSDM deposit of the northern ECS (Fig. 7).

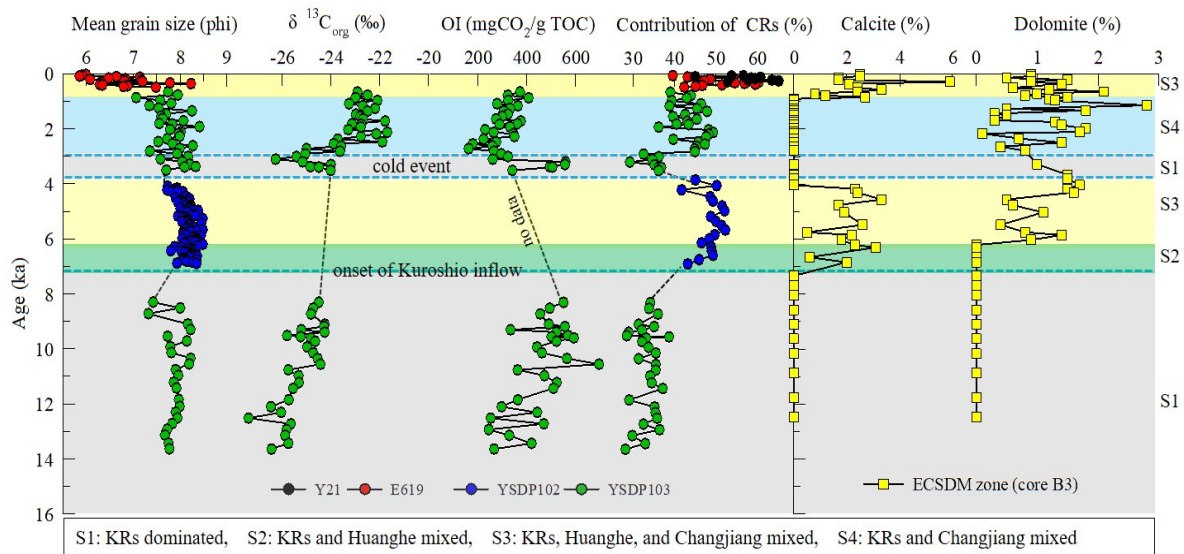


**Figure 7.** Downcore variations of mean grain size, carbon isotopic ratio ( $\delta^{13}\text{C}_{\text{org}}$ ), oxygen index (OI), and quantitative contribution of the CRs in the SEYSM deposit during the last 15 kyr and comparison with records of calcite-dolomite contents (Hu et al., 2014) in the ECSDM deposit. The four cores from the SEYSM were combined into one continuous record based on a composite chronology.

Overall, our result depicts a clear sedimentation trend over the course of the Holocene, marked by a large increase in the CR contribution since  $\sim 7$  ka, with a sudden decline at  $\sim 3\text{--}4$  ka, which seems to parallel other geochemical compositions ( $\delta^{13}\text{C}_{\text{org}}$ , and OI) of the SEYSM deposit, as well as carbonate mineral components of the ECSDM deposit (Fig. 7). It is intriguing to note that the SEYSM deposit was filled mainly with the KR-sourced sediments ( $\sim 80\%$  of contribution) before  $\sim 7$  ka; thus, terrigenous matter supplies from adjacent Korean rivers would have predominantly contributed to the deposit during this period. Also, low  $\delta^{13}\text{C}_{\text{org}}$  ( $< -24\text{‰}$ ), and high OI ( $> 400 \text{ mgCO}_2/\text{g TOC}$ ) values indicate that this deposit with rich terrestrial organic matters was formed under a freshwater-dominated depositional environment (Stein, 1991; Ruttenberg and Goni, 1997; Kong et al., 2006). Additionally, a gradual increase in  $\delta^{13}\text{C}_{\text{org}}$  implies a diminutive supply of terrestrial organic materials resulting from hydrological changes, such as a retreat of rivers led by the postglacial sea-level rise and flooding of the shallow shelf. It



is interesting to note that the complete absence of carbonate minerals in the ECSDM deposit is likely to reflect no supply of the CR sediments to the northern ECS shelf during the time period in question (Fig. 7). Considering modern sediment transport dynamics, as discussed above, the absence of carbonate is probably a result of combined effects a lack of transport media (no YSWC and YSCC) in the YECSs and distally located river mouths that would have been positioned significantly closer to the present day's outer shelf. This conclusion is supported by previous studies demonstrating that the YECS deposit formed during the Holocene transgression period consisted of terrigenous sediments from adjacent rivers and/or reworked and resuspended sediments of exposed shelf deposits (e.g., Saito et al., 1998; Yoo et al., 2002; Uehara and Saito, 2003; Yang and Youn, 2007; Hu et al., 2014; Dou et al., 2015).

A sudden and very distinct increase in the CR source contribution since ~7 ka may be induced by an intrusion of the YSWC to the study area, resulting in a significant CR sediment supply to the Korean coastal zone. This assumption can also be drawn from the large increase in  $\delta^{13}\text{C}_{\text{org}}$  values that suggests increased marine planktonic organisms owing to more open-marine conditions (Fig. 7). In the ECSDM core, simultaneously, a prominent increase in the carbonate mineral contents implies a massive input of both Huanghe and Changjiang sediments to the northern ECS shelf and even Korean coastal zones, which is in line with the idea of YSWC intrusion under a fully developed oceanic environment by that time. What also becomes apparent is that this event corresponds to the time point initiating a delivery of fine-grained Changjiang sediments to the northern ECS by the southwestward YSCC in winter and/or the northeastward Changjiang Diluted Water (CDW) in summer (Yang et al., 1992; Zhang, 1999; Lie et al., 2003; Liu et al., 2007; Yuan et al., 2008; Zhang et al., 2019) as well as a transport of the old-Huanghe deltaic sediments to the northeastern ECS by the YSCC, resulting in the ECSDM formation. This justifies the previous notion that the paleo-Huanghe

flowed through the North Jiangsu Plain, by which the sediment loads were carried and eventually delivered to the ECSDM by the southeastward YSCC (Yang et al., 2003; Hu et al., 2014; Lim et al., 2015a). Further, since ~7 ka, the Changjiang sediments were delivered to the ECSDM by the southeastward YSCC in winter and/or the northeastward CDW in summer (Milliman et al., 1985, 1986; Yang et al., 1992; Naimie et al., 2001; Lie et al., 2003; Yuan et al., 2008; Moon et al., 2009). As expected, the marked shift in the sediment source that began at ~7 ka provides a clear evidence of how the modern coastal-shelf sediment delivery system had stabilized by that time.

The tentative link between the sediment source variation and the YSWC inflow is also evident in an abrupt weakening of the CR contribution to the mud patches during a short time interval in the late Holocene (ca. ~4–3 ka, Fig. 7). As suggested earlier, the diminished CR sediment deposition during this period is likely to be resulted from a weakening of the YSWC and YSCC inflow and thus, deteriorated particle transportation ability of the currents carrying the CR source materials from the northern ECS to the YECSs. A remarkable decrease in  $\delta^{13}\text{C}_{\text{org}}$ , and increase in OI (Fig. 7), which indicates a significantly increased freshwater discharge under deteriorated oceanic condition, provides additional evidence to support this claim. These prospects further justify the late Holocene neoglacial cold event (i.e., the *Pulleniatina* minimum event, ~5–3 ka) documented in the northwestern Pacific marginal seas (e.g., the ECS and Okinawa Trough, Kim and Lim, 2014 and references therein; Lim et al., 2017; Xu et al., 2019), led by the suppression of the Kuroshio system (Jian et al., 2000; Xiang et al., 2007).

From a climatic point of view, there are several terrestrial aspects that may have exerted a crucial role in destabilizing the sediment source variations for this particular time interval. A recent study confirms that this abrupt cold episode (i.e., a 3–4°C drop in sea surface temperature) was considerably affected by a global climatic transition called the “4.2-ka event”, which also have transformed the East

Asian monsoon hydrological regime (Kajita et al., 2018; Park et al., 2019). During this interval, high eolian dust flux into the YECSs shows another climatic response, such as an intensification of East Asia winter monsoon (Lim et al., 2005; Lim and Matsumoto, 2008). We speculate that this cold episode was severe enough to damage the oceanic circulation system (especially the Kuroshio Current), leading to a plausible explanation for the abrupt interruption of the CR sediment supply to the YECSs. Indeed, the short waning stage of the CR sediment input to the YECSs is coeval in time with a terrestrial cooling-dry episode in northern China, as well as a weakened Kuroshio influence and an intensified winter monsoon; thus, this finding emphasizes the significance of oceanic-atmospheric interactions in determining moisture and heat distributions over both oceanic and terrestrial domains (Kim and Lim, 2014; Huang et al., 2016; Kajita et al., 2018; Xu et al., 2019). Another issue is that, similar to that of the sea level lowstand, the sudden decrease in the CR sediment supplies to the northern ECS appears to be caused by a suppression of the northward YSWC during this time period. The overall synchronicity between these sediment source variations and oceanic circulation changes in the northwestern Pacific (including the YECSs) during the mid-to-late Holocene is very obvious and apparently depicts a global climate signal, not just solely regional climatic processes.

After this short cold event, a marked change in the CR sediment contribution and organic geochemical records increased  $\delta^{13}\text{C}_{\text{org}}$  ( $> -23\text{‰}$ ), and decreased OI (200–400 mg  $\text{CO}_2/\text{g}$  TOC) may primarily reflect a re-development of the oceanic environment, indicating a restoration of the YSWC inflow. Interestingly, despite the overall good comparability between the Changjiang and Huanghe source contributions into the ECSDM, there were some significant differences after the late Holocene cold event (Fig. 7); whereas the Changjiang sediments were resupplied to the northern ECS continuously ( $\sim 3$  ka), the Huanghe source curve remained rather muted until  $\sim 1$  ka. The disappearance of the Huanghe sediments

during the time interval ( $\sim 3$ – $1$  ka) may be related to a massive drainage transformation in China (i.e., shifting of the Huanghe course towards the Bohai Sea) and resultant climatic and anthropogenic changes around the river basin (Hu et al., 2014 and references therein), which would have restricted the Huanghe source inputs to the YECSs (Li et al., 2014b; Yang and Liu, 2007; Bian et al., 2010; Hu et al., 2011). Meanwhile, the later period (after  $\sim 1$  ka) is an interesting case; the maximal CR source contribution to the SEYSM and ECSDM deposits with a sudden increase in the Huanghe sediment supply (Fig. 7) is synchronous with intense human interventions around the Changjiang and Huanghe basins. These interventions profoundly increased the sediment load after  $\sim 2$  ka, from  $\sim 240$  to  $\sim 480$  Mt/yr in Changjiang and from 500 to  $\sim 1,200$  Mt/yr in Huanghe (Milliman et al., 1987; Ren and Zhu, 1994; Hori et al., 2001; Wang et al., 2007, 2011). The sharply increased sediment supply from the two rivers since  $\sim 1$  ka would have further facilitated fine-grained sediment transport to the YECSs. This assumption gains further support from a recent finding that offshore erosion in the paleo-Huanghe delta produces more than 790 Mt/yr of sediments, and almost half of the sediment load is transported southeastward to south of Cheju Island in the northern ECS (Zhou et al., 2014). Considering all of the above, implementation of our Mg/Al regression model to the two sedimentary archives (SEYSM and ECSDM deposits) successfully produces a reasonable paleoenvironmental interpretation on the compiled marine-terrestrial data around the northwestern Pacific margin, and hence beholds its pivotal role in studies of provenance reconstructions globally.

## 6. Conclusions

In this study, we analyzed the Al and Mg contents of 399 surface sediments from the coastal and shelf zones of the YECSs and 14 sediment cores ( $n = 310$  subsamples) from the several mud patches to illustrate spatiotemporal variations of

the sediment sources and elucidate their major controlling mechanisms. Notably, the correlation of Mg with Al displays different linear regression trends for KR and CR sediment groups, enabling the source areas to be differentiated more clearly in the YECSs. For quantifying the sediment sources, we improved Al-Mg regression analysis by correcting and re-calculating these two linear regression lines. This approach involves the effective normalization of bulk contents to account for differences of grain size in sediment geochemistry, which would enable more unequivocal sediment source discrimination in the YECSs. The results successfully described spatiotemporal variations in quantitative source apportionments, yielding a broader understanding of source-to-sink dynamics, especially on the CYSM and SEYSM deposits. Spatial distribution, particularly a sudden decrease of CR contribution around 124°E, may be controlled by a unique role YSCWM, coupled with the bathymetry, YSWC, and a strong tidal front. Quantitative estimates revealed that the proportion of CR sediments ranged from 30 to 40% in the SEYSM and that of KR sediments is up to 50%. In terms of its application to historic sedimentary deposits of the YECS sediments over the last 15 kyr, our fingerprint-inferred provenance changes depict a clear sedimentation trend over the course of the Holocene, marked by a large increase in the CR contribution since ~7 ka, with a sudden decline at ~3–4 ka, which seems to parallel other geochemical compositions ( $\delta^{13}\text{C}_{\text{org}}$ , and OI) of the SEYSM deposit, as well as carbonate mineral components of the ECSDM deposit. Subsequently, the strong spatiotemporal coherence in the YECS sediment source quantifications validates our approach, which may potentially benefit more robust constraints on sediment source-to-sink studies in a variety of contexts and application.

# Chapter 3



REE fractionation and sediment  
source quantification

## 1. Research background

As gateways to the open ocean and sensitive filters for terrigenous matter inputs dispersing into marginal seas, continental margins bear strong imprints of complex land–ocean processes. Therefore, investigating sediment delivery from the source terrain to the ultimate sink may elucidate not only the overall fluvial sediment dispersal systems but also the mechanisms responsible for transferring environmental variabilities due to climatic and anthropogenic forcings, particularly in shelves with multiple sediment sources. The Yellow Sea, which has the world’s highest sediment loads (~10% of the world’s fluvial sediment discharge, Milliman and Meade, 1983), has been noted as an ideal benchmark region for this purpose, with its multiple riverine sediment sources and complex interconnectivity of coastal-shelf current systems. In particular, the unique shelf-mud deposit patches of the Holocene depositional systems in the river-dominated Yellow Sea shelf (Fig. 1) have received considerable attention because they are active sedimentary depocenters that link sediment sources, transports, and sinks; thus they can elucidate the river sediment dispersal patterns and the depositional systems of the entire Yellow Sea (Lee and Chough, 1989; Alexander et al., 1991; Lim et al., 2007; Gao and Collins, 2014; Wang et al., 2014; Zhou et al., 2015; Qiao et al., 2017; Lee et al., 2020 and references therein). However, the sediment source-to-sink systems of these shelf-mud deposits are still not well understood. For example, the dispersal limit and quantitative contribution of river sediments in the distal mud deposit of the central Yellow Sea (CYSM) and the coastal mud belt of the southeastern Yellow Sea (SEYSM or Huksan mud belt) remain highly controversial (e.g., Park et al., 2000; Lim et al., 2007, 2015a; Lee, 2015; Koo et al., 2018; Lee et al., 2020). This may stem from the lack of a reliable source discrimination model that can quantify contributions of riverine sediments in the Yellow Sea, which would provide significant insights into the complex interactions among single or multiple fluvial sources and hydrodynamic processes.

Efforts over past decades have focused on the development of mineralogical and geochemical proxies to identify the source of sediments in the Yellow Sea (e.g., Lee et al., 1992; Cho et al., 1999; Park and Khim, 1992; Yang et al., 2003a and reference therein; Lim et al., 2006, 2015a), but these studies may be inappropriate and result in completely different conclusions regarding source identification. Yang et al. (2003a) concluded that most previous suggestions and proxies of sediment provenance in the Yellow Sea are not coincident and/or are sometimes even contradictory. This may be due to the grain-size and compositional fractionation effects on elemental concentrations of bulk sediments (Lim et al., 2006, 2015a; Jung et al., 2014, 2016a, 2016b). Although rare earth elements (REEs) are trustworthy tracers for sediment source studies because of their highly conservative behavior during Earth surface processes (e.g., McLennan, 1989; Sholkovitz, 1990; Singh and Rajamani, 2001; Prego et al., 2009), their concentrations are also vulnerable to grain size effects (GSEs) and change during transport processes (Yang et al., 2003b; Feng et al., 2011; Zhang et al., 2012; Lim et al., 2014; Jung et al., 2016b). To ameliorate this deficiency and discriminate clearly between Chinese (CRs) and Korean river (KRs) sediments in the Yellow Sea sediments, a REE proxy based on the grain size and/or chemical partitioning analyses of riverine sediments was recently suggested (Song and Choi, 2009; Lim et al., 2014). However, the fractionation characteristics of REEs both in different grain size fractions and chemical species of bulk sediments in the Yellow Sea are not understood adequately to quantify the proportional contributions of source sediments in the Yellow Sea mud deposits.

To better constrain geochemical links of mud deposits to source rocks and provide more robust insights on their origins, we analyzed REE concentrations both in granulometrically and chemically partitioned fractions of the bulk sediments from CRs and KRs and two shelf-mud deposits (CYSM and SEYSM). REE fractionation patterns with respect to grain size fractionation and chemical speciation were



considered and mathematically formulated to develop a noble REE-source model applicable to the Yellow Sea mud deposits. This new model including grain size compensation may elucidate the source-to-sink system of shelf-mud deposits in the Yellow Sea affected by multiple sources (i.e., KR and CR) and complex current systems.

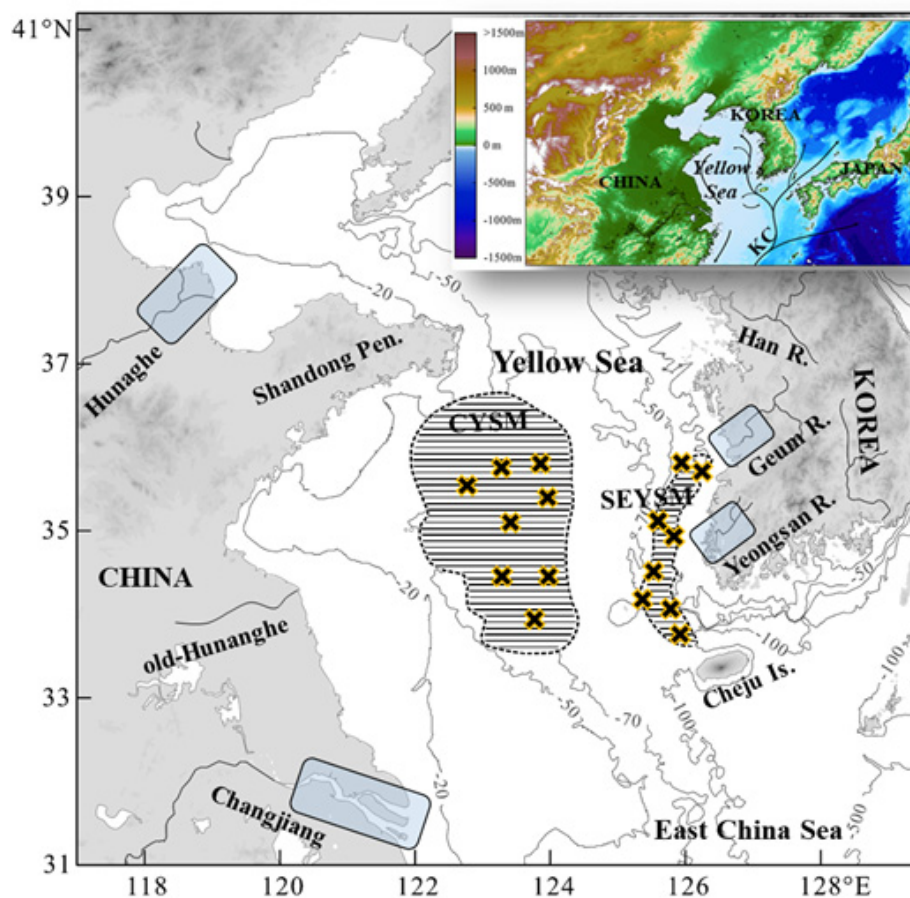


Figure 1. Map of the study area including the sediment sampling areas (shaded) in Chinese (Huanghe and Changjiang) and Korean (Geum and Yeongsan Rivers) rivers and sampling sites (x marks) in the shelf-mud patches (CYSM: Central Yellow Sea Mud, SEYSM: Southeastern Yellow Sea Mud).

## 2. Materials and analytical methods

A total of 47 surface sediments were collected from the mouths of KRs (Geum and Youngsan Rivers) and CRs (Huanghe and Changjiang) and two shelf-mud deposits (CYSM and SEYSM) (Fig. 1). All sediments were granulometrically and chemically partitioned to constrain the REE concentrations. The sediments were first fractionated into two subpopulations (silt population of 20–60  $\mu\text{m}$  and clay population of  $<20$   $\mu\text{m}$ ) using the classic sieving technique and then dried and powdered in an agate mortar. To measure total concentrations of REEs,  $\sim 0.2$  g each grain size population was weighed, placed into a graphite crucible, and blended with 1.0 g lithium metaborate ( $\text{LiBO}_2$ ). Then the combined powders were fused at 900  $^\circ\text{C}$  for 20 min, and the resultant cake was cooled and dissolved in 200 mL cold 5% nitric acid ( $\text{HNO}_3$ ). Each solution was analyzed for REE concentrations using inductively coupled plasma mass spectrometry (ICP-MS) at the University of London. The validity of the analytical procedure was evaluated for accuracy and precision using the reference sample MAG-1 ( $n = 12$ ). The accuracy and precision for most elements were generally  $\leq 10\%$ , indicating satisfactory recoveries.

The powdered samples ( $\sim 0.2$  g) were leached with 20 mL 1 N hydrochloric acid (HCl) for 24 h at room temperature (Yang et al., 2004; Song and Choi, 2009) and then the supernatants (solutions) after centrifugation were analyzed for acid leachable concentrations of REEs using ICP-MS at the Korea Basic Science Institute (KBSI) in Daejeon, Korea. Analytical uncertainty based on the reference sample MAG-1 ( $n = 10$ ) was  $\leq 10\%$  for the leachable concentrations, similar to that in the total REE concentration analyses. The REE concentration of the residual fraction was defined as the difference between the total and HCl-leached fraction. The leached fraction is expected to contain adsorbed parts, amorphous Fe–Mn oxides, carbonate minerals, crystalline iron oxides, authigenic and detrital apatite, and some weathered detrital/clay components (Cronan and Hodkinson, 1997;

Mascarenhas-Pereira and Nath, 2010; Su et al., 2017). Regarding aluminum (Al), the partial dissolved amounts of detrital aluminosilicate (mainly chlorite) materials in the 1 N HCl-leached fraction were  $\leq 10\%$  (Lim et al., 2014). The residual fraction contained mainly resistant silicates, aluminosilicates, and heavy minerals that were insoluble in 1 N HCl solution, along with some heavy minerals.

### **3. Fractionation distribution characteristics of REE partitioning**

The analytical results of the grain size (silt and clay populations) and chemical (HCl-leached and residual fractions) partitioning experiments for the riverine and shelf sediments from the Yellow Sea are summarized in Table 1. The average relative percentages of the acid-leached fraction in the clay population were 54%, 47%, 43%, and 47% in KR, CR, SEYSM, and CYSM, respectively; the percentages for most REEs range from 40% to 60% in all sediment groups, except for Gd (60–70%) and Yb and Lu (30–40%). In the silt population, the average percentages were 35%, 28%, 27%, and 24% in KR, CR, SEYSM, and CYSM, respectively; the percentages ranged from 25% to 40%, except for Gd (35–45%) and Yb and Lu (15–20%). Acid-leachable REEs were slightly more abundant in KR sediments and in the clay population.

Fractionation characteristics of the upper continental crust (UCC)-normalized REE ( $REE_{UCC}$ ) distribution pattern in riverine sediments have been discussed as a potential proxy for sediment source discrimination in the Yellow Sea (Jung et al., 2006, 2012, 2016b; Song and Choi, 2009; Xu et al., 2009; Lim et al., 2013, 2014; Um et al., 2015). For example, in the  $REE_{UCC}$  fractionation distribution of bulk sediments, light-REEs (La to Nd) are more abundant than heavy-REEs (Ho to Lu) in KR sediments; therefore, the REE distribution pattern of KR sediments shows a decreasing trend from light- to heavy-REEs. However, middle-REEs (Sm to Dy) are more highly concentrated than light- and heavy-REEs in CR sediments, resulting in a convex shape in the fractionation distribution pattern.

Table 1. Descriptive statistics (average, standard deviation and range) of REE concentrations ( $\mu\text{g/g}$ ) for the granulometrically and chemically partitioned riverine and shelf sediments of the Yellow Sea. CRs: Chinese rivers, KRs: Korean rivers, CYSM: Central Yellow Sea Mud, SEYSM: Southeastern Yellow Sea Mud.

Sediment group	La	Ce	Pr	Nd	Sm	Eu	Gd	Dy	Ho	Er	Yb	La			
CRs and KRs: Chinese and Korean rivers, CYSM: Central Yellow Sea Mud deposits, SEYSM: Southeastern Yellow Sea Mud deposits	population	CRs (n=18)	15.08±1.71 (11.26-18.28)	32.83±3.92 (23.06-38.50)	3.95±0.42 (2.87-4.60)	15.81±1.66 (11.42-17.99)	3.51±0.38 (2.51-4.00)	0.72±0.10 (0.49-0.83)	3.28±0.34 (2.37-3.71)	2.42±0.26 (1.76-2.74)	0.45±0.05 (0.32-0.51)	1.15±0.13 (0.81-1.30)	0.90±0.10 (0.65-1.03)		
		Landshel fraction	KRs (n=13)	28.68±7.07 (15.75-38.26)	58.60±13.52 (31.13-81.00)	6.62±1.40 (4.09-8.56)	24.61±4.76 (16.05-31.17)	4.76±0.79 (3.48-5.83)	0.96±0.15 (0.71-1.17)	3.99±0.56 (3.18-4.83)	2.94±0.44 (2.32-3.35)	0.54±0.09 (0.41-0.66)	1.39±0.25 (1.04-1.72)	1.10±0.20 (0.80-1.36)	0.15±0.03 (0.11-0.19)
			SEYSM (n=6)	18.62±1.35 (15.87-20.54)	39.10±3.01 (32.84-42.90)	4.54±0.32 (3.88-4.98)	17.48±1.23 (14.92-18.99)	3.60±0.38 (2.99-3.86)	0.72±0.06 (0.59-0.79)	3.16±0.22 (2.69-3.58)	2.34±0.16 (2.01-2.33)	0.43±0.03 (0.37-0.47)	1.09±0.07 (0.95-1.18)	0.85±0.07 (0.70-0.93)	0.12±0.01 (0.10-0.13)
		CYSM (n=6)	15.76±0.87 (14.54-16.80)	34.76±1.95 (31.80-37.22)	4.07±0.19 (3.81-4.33)	16.05±0.64 (15.17-16.92)	3.52±0.14 (3.38-3.80)	0.72±0.01 (0.71-0.74)	3.19±0.08 (3.10-3.37)	2.32±0.07 (2.27-2.49)	0.42±0.01 (0.41-0.44)	1.05±0.04 (1.02-1.14)	0.82±0.02 (0.80-0.85)	0.11±0.00 (0.11-0.12)	
	Clay	CRs (n=18)	22.60±4.32 (15.31-32.57)	45.44±10.14 (29.48-69.95)	4.47±0.95 (2.81-7.01)	19.61±3.76 (13.15-29.48)	3.04±0.78 (1.77-5.04)	0.66±0.14 (0.37-0.92)	1.51±0.66 (0.58-3.08)	2.32±0.63 (1.32-3.84)	0.50±0.11 (0.33-0.76)	1.44±0.35 (1.03-2.22)	1.76±0.29 (1.37-2.52)	0.28±0.08 (0.19-0.45)	
		Landshel fraction	KRs (n=13)	24.31±2.55 (20.57-29.27)	47.58±6.98 (39.32-61.01)	4.74±0.62 (4.15-5.84)	22.34±2.73 (19.60-27.03)	3.30±0.45 (2.45-3.98)	0.64±0.12 (0.42-0.86)	1.66±0.32 (1.31-2.18)	2.27±0.27 (1.80-2.79)	0.48±0.08 (0.30-0.60)	1.34±0.15 (1.12-1.62)	1.73±0.14 (1.56-2.02)	0.26±0.03 (0.20-0.30)
			SEYSM (n=6)	27.35±4.26 (21.61-32.95)	55.29±8.92 (42.25-66.16)	5.56±0.82 (4.55-6.84)	24.45±3.68 (19.17-29.82)	3.99±0.72 (3.15-4.43)	0.73±0.12 (0.57-0.89)	2.02±0.53 (1.49-3.06)	2.62±0.45 (1.93-3.34)	0.54±0.08 (0.43-0.65)	1.50±0.25 (1.22-1.94)	1.92±0.26 (1.43-2.38)	0.31±0.04 (0.26-0.36)
		CYSM (n=6)	23.84±2.30 (20.63-26.71)	46.85±4.38 (41.38-52.60)	4.69±0.31 (4.26-5.09)	20.03±0.95 (18.41-21.06)	3.14±0.28 (2.82-3.56)	0.59±0.06 (0.48-0.66)	1.52±0.24 (1.25-1.86)	2.05±0.25 (1.68-2.37)	0.48±0.03 (0.36-0.46)	1.30±0.13 (1.05-1.48)	1.62±0.14 (1.40-1.78)	0.26±0.02 (0.22-0.28)	
	Silt	CRs (n=12)	7.19±0.73 (6.12-8.76)	14.12±1.60 (11.91-17.56)	1.82±0.17 (1.61-2.22)	7.22±0.66 (6.43-8.73)	1.57±0.15 (1.35-1.89)	0.30±0.02 (0.27-0.36)	1.48±0.15 (1.24-1.79)	1.09±0.11 (0.91-1.31)	0.20±0.02 (0.17-0.25)	0.52±0.07 (0.44-0.66)	0.40±0.05 (0.34-0.50)	0.06±0.01 (0.05-0.07)	
		Landshel fraction	KRs (n=12)	10.64±4.13 (6.64-21.82)	21.87±10.63 (12.90-50.70)	2.41±0.98 (1.31-5.09)	9.02±3.67 (5.09-19.21)	1.75±0.70 (1.14-3.76)	0.34±0.16 (0.23-0.80)	1.46±0.60 (0.99-3.19)	1.04±0.44 (0.68-2.32)	0.13±0.08 (0.13-0.42)	0.49±0.20 (0.32-1.08)	0.40±0.17 (0.25-0.89)	0.05±0.02 (0.03-0.12)
			SEYSM (n=7)	7.02±0.45 (6.48-7.33)	13.33±0.83 (12.18-14.37)	1.66±0.09 (1.54-1.77)	6.31±0.40 (5.75-6.80)	1.27±0.09 (1.14-1.38)	0.24±0.02 (0.21-0.26)	1.09±0.08 (0.97-1.19)	0.79±0.07 (0.69-0.89)	0.14±0.01 (0.12-0.16)	0.37±0.03 (0.32-0.41)	0.28±0.03 (0.24-0.32)	0.04±0.00 (0.03-0.04)
		CYSM (n=4)	6.87±0.93 (6.28-8.26)	14.05±1.77 (13.11-16.70)	1.73±0.22 (1.61-2.06)	6.82±1.00 (6.24-8.31)	1.47±0.18 (1.33-1.73)	0.27±0.02 (0.25-0.29)	1.33±0.17 (1.19-1.57)	0.96±0.11 (0.87-1.12)	0.18±0.02 (0.16-0.21)	0.45±0.05 (0.41-0.51)	0.35±0.04 (0.31-0.40)	0.05±0.01 (0.04-0.06)	

The different distribution patterns between CR and KR sediments are well-known qualitative REE<sub>UCC</sub> fractionation characteristics (Xu et al., 2009; Jung et al., 2012; Lim et al., 2014 and references therein). Thus, systematic variation in the REE fractionation parameters including (light-REE/heavy-REE)<sub>UCC</sub> ratio, and (La/Yb)<sub>UCC</sub>–(Gd/Yb)<sub>UCC</sub>, (La/Lu)<sub>UCC</sub>–(La/Y)<sub>UCC</sub>, and (La/Y)<sub>UCC</sub>–(Gd/Lu)<sub>UCC</sub> relations have been considered with the greatest discriminatory power (Yang et al., 2002, 2003b; Jung et al., 2006, Xu et al., 2009; Lim et al., 2013; Um et al., 2015). However, these simple ratios between REEs have not been examined critically, particularly regarding the GSEs, which cannot represent an entire fractionation distribution pattern of all REEs. This has frequently resulted in inadequate interpretations of the sources, particularly for the bulk sediments (Lim et al., 2014; Jung et al., 2016b).

To better compare the REE fractionation characteristics of riverine sediments under free-GSE conditions, Jung et al. (2016b) proposed the use of a standardized REE value ( $[(\text{REE}_{\text{UCC}})_{\text{STD}}]$ ). The value is standardized by re-drawing the fractionation distribution after dividing the UCC-normalized values of each REE by an average value of the UCC-normalized ratios of REEs (Eq. 1). Thus, the total sum of the  $(\text{REE}_{\text{UCC}})_{\text{STD}}$  value (hereafter “SREEs”) for 12 REEs should be 12:

$$\sum_{i=La}^{Lu} \left( \frac{C_i}{\left( \frac{\sum_{j=La}^{Lu} C_j}{n} \right)} \right) = 12 \quad (\text{Eq. 1})$$

$C_{i(\text{or } j)}$ : UCC-normalized concentration ratio of REE (i or j);  $n = 12$  (number of i (or j))

Following this correction, REE concentrations are first standardized for all sediment samples, and fractionation patterns of SREE values are characterized to better define the difference between the distribution patterns of the CR and KR sediments and the SEYSM and CYSM deposits (Fig. 2).

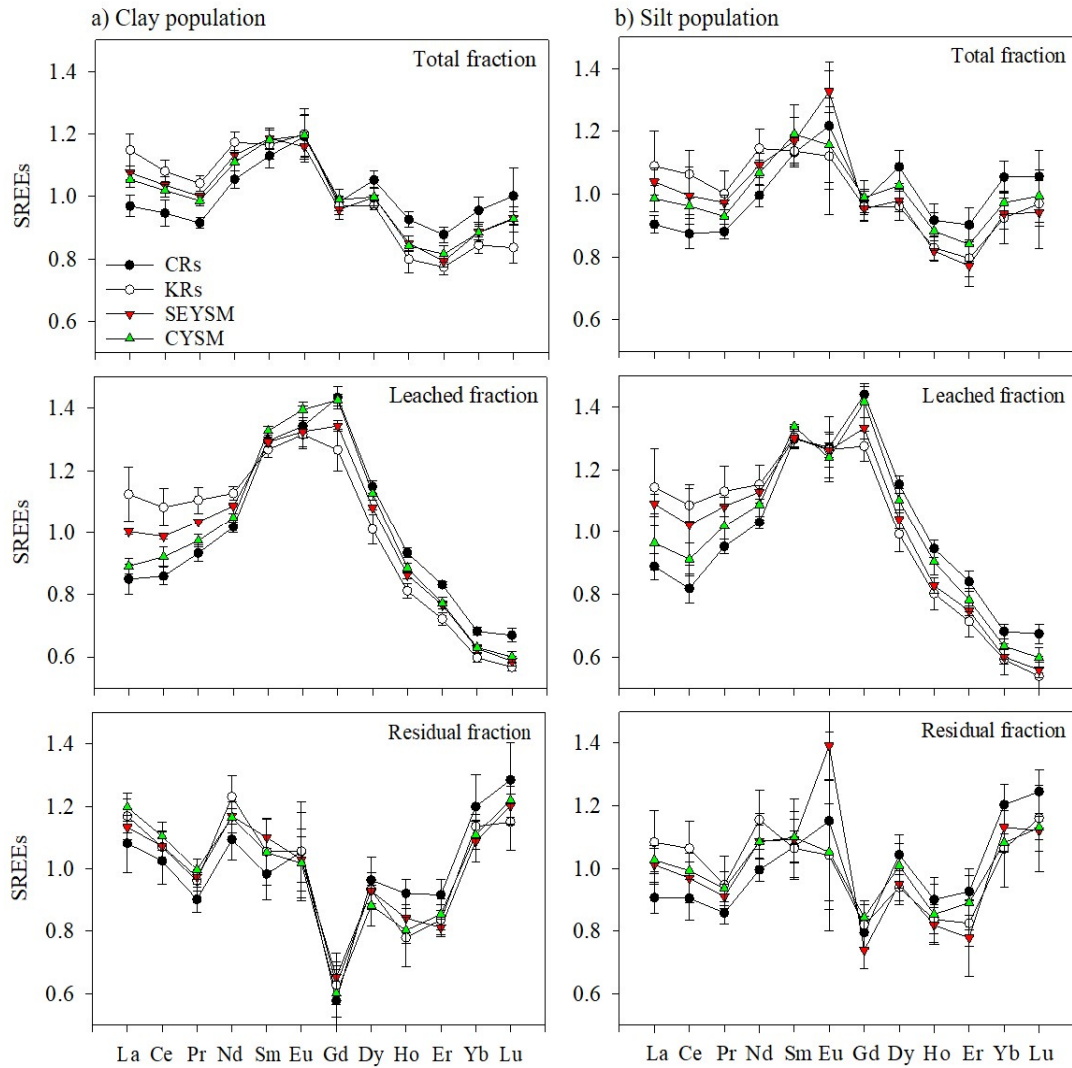


**Figure 2.** Fractionation distributions of average SREE (standardized REE value,  $[(REE_{UCC})_{STD}]$ ) values for the clay (a) and silt (b) populations of riverine and shelf mud sediments. Note that KR sediments are relatively enriched in light-SREEs but depleted in heavy-SREEs compared to CR sediments, particularly in the leached fractions of grain size populations. CRs: Chinese rivers, KR: Korean rivers, CYSM: Central Yellow Sea Mud, SEYSM: Southeastern Yellow Sea Mud.

In the clay (< 20  $\mu\text{m}$ ) and silt (20–60  $\mu\text{m}$ ) populations of all riverine and shelf sediments, the overall SREE values in the acid-leached fraction exhibited a remarkably high enrichment of middle-REEs and a strong depletion of heavy-REEs, with intermediate light-REEs (Fig. 2). This qualitative REE<sub>UCC</sub> fractionation distribution is well known in riverine sediments around the Yellow Sea (Xu et al., 2009; Lim et al., 2013, 2014; Jung et al., 2016b). Such a pronounced middle-REE enrichment signature in the leached fraction of CR and KR sediments may be linked to Fe-oxide minerals (e.g., Fe oxyhydroxide, ferrihydrite, lepidocrocite, and goethite), with minor apatite and carbonate fractions (Palmer, 1895; Yang et al., 2002; Song and Choi, 2009; Zhang and Gao, 2015). In the Yellow Sea shelf mud sediments, the middle-REE enrichment reflects the inherent properties of riverine sources, and may be due to the complex ability of REEs with several kinds of carboxylic acids which roughly follow convex shapes (Wang et al., 1994; Zhang et al., 1998). In addition, the light-SREE values in the leached fractions of the silt and clay populations varied systematically between the sediment groups of this study; the values were highest in the KR sediments, followed by SEYSM, CYSM, and CR sediments (Fig. 2). Relatively high concentrations of leached light-REEs in KR sediments are most likely related to clay minerals (particularly chlorite) (Song and Choi, 2009).

In the residual fraction of the clay population, fractionation distribution patterns of the SREEs were characterized by slight enrichment of light- and middle-REEs (La to Dy), except for Gd with the lowest value, and Yb and Lu with the highest values (Fig. 2). The light- and middle-SREE enrichments in the residual fractions were much higher in the KR sediments than in the CR sediments, which may be due to the difference in bulk mineralogical compositions of source rocks of the KR (mostly granites) and CR sediments (mostly granodioritic composition with abundant mafic minerals) (Jung et al., 2012; Lim et al., 2014, 2015a). In the silt population, meanwhile, the distribution of the residual

SREEs did not show any noticeable pattern (Fig. 2). Except for Lu in the CR sediments, the SREE values were in the range between 0.8–1.2 without any systematic distribution pattern, such as light- and middle-REE enrichment. This may have been due to the enrichments of light- and/or heavy-REEs of refractory heavy minerals, which are abundant in the residual fraction of the silt population (Yang et al., 2002; Jung et al., 2012, 2016b; Lim et al., 2014). Heavy mineral contents in the shelf sediments can be constrained by mineralogical sorting associated with hydrodynamic conditions during transport and depositional processes (Lee et al., 1988; Wang et al., 2010; Li et al., 2017), suggesting that REE concentrations of the residual fractions should be used with caution as a sediment proxy.

In the total fraction of both the silt and clay populations, general SREE fractionation distribution patterns were similar to (although flatter than) those of the leached fraction (Fig. 2). The distribution patterns were relatively high in middle-REEs, followed by light- and heavy-REEs, although the magnitudes were relatively low compared to those of the leached fractions. This was due to dilution caused by the significant amount of the leached fraction (Table 1).

#### **4. New source discrimination model using REE fractionation distribution**

The middle-SREE enrichment and heavy-SREE depletion were notable features in the fractionation distribution, particularly in the leached fractions in all grain size populations (Fig. 2). In addition, the values of light-SREEs in the leached and total fractions varied widely among the sediment groups; KR sediments were the highest, followed by SEYSM, CYSM, and CR sediments. To better recognize such differences between sediment groups, the SREE values were normalized with the average SREE value of the CR sediments. Interestingly, the CR-normalized SREE (hereafter “SREE<sub>CR-n</sub>”) values in all grain size and chemical partitions decreased linearly with atomic number from La to Lu ( $r^2 > 0.8$ ; Fig. 3).



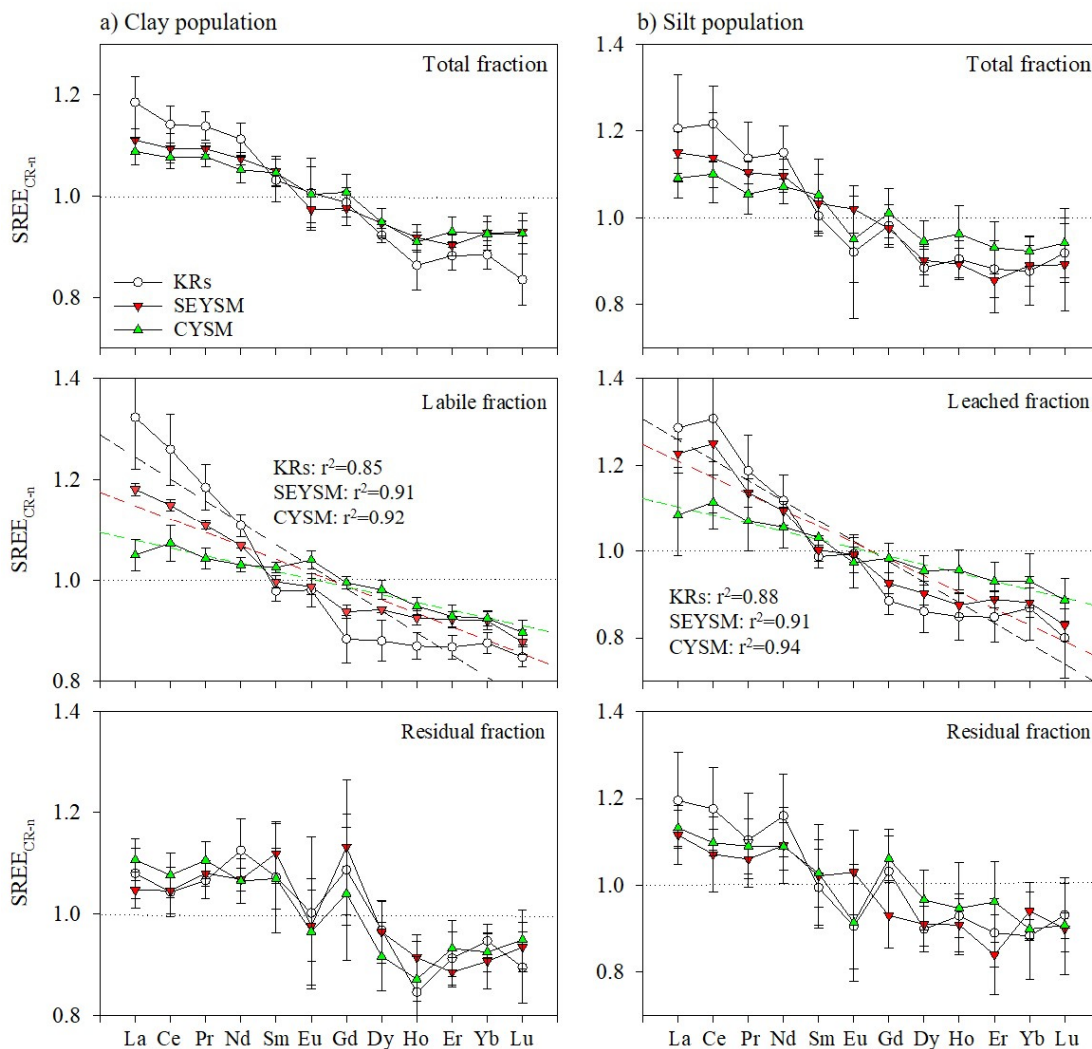


**Figure 3.** Fractionation distribution patterns of CR-normalized SREEs ( $SREE_{CR-n}$ ,  $[SREE/SREE_{CR}]$ ) values for the clay (a) and silt (b) populations of KR and shelf mud sediments. Note that the linear regression line (i.e., the slope value) of each sediment group in the  $SREE_{CR-n}$  distribution patterns indicates similarity to CR sediments in REE compositional properties. Interestingly, the slopes show strong correlation ( $r^2 \geq 0.8$ ) and are most clearly distinguished in the leached fractions. CRs: Chinese rivers, KR: Korean rivers, CYSM: Central Yellow Sea Mud, SEYSM: Southeastern Yellow Sea Mud.

In addition, the slopes of the linearly decreasing trends differed largely in each sediment group; the slope was steepest in KR sediments, followed by those of SEYSM and then CYSM, with a significant prominence in the leached clay fraction. Thus, the difference in  $SREE_{CR-n}$  fractionation distribution patterns between the sediment groups can be numerically represented as the slope of the linear regression. This reflects the intensity of light-REE enrichment and heavy-REE depletion; that is, the slope value of the regression line indicates the similarity to CR sediments in terms of REE compositional properties. The results clearly showed that the value of the slope decreased in order of CR, CYSM, SEYSM, and KR sediment groups, although they were somewhat scattered with wide error ranges, particularly in the silt fraction (Figs. 3 and 4). KR sediments, one of the major source end-members in the Yellow Sea, had the highest slope value, suggesting that their REE compositions (particularly light- and heavy-REEs) differ significantly from those of CR sediments. Several studies have shown that the difference in REE composition between KR and CR sediments is closely linked to the parent rocks (Lim et al., 2014, 2015b). The pronounced enrichment of light-REEs and depletion of heavy-REEs in KR sediments is attributed to their greater felsic compositions with more abundant silicate contents compared to CR sediments or the UCC of granodiorite compositions with relatively more abundant mafic minerals (e.g., plagioclase and biotite mica). In general, more silicic rocks contain higher light-REE/heavy-REE ratios because the concentration of light-REEs in felsic rocks tends to increase relative to the heavy-REE concentration (e.g., Cullers and Graf, 1983; Nyakairu and Koeberl, 2001; Sanematsu et al., 2009). As a result, the slope value for  $SREE_{CR-n}$  fractionation distribution pattern may be a more effective proxy for distinguishing KR sediments from CR sediments in the Yellow Sea.

Meanwhile, the slope values for CYSM and SEYSM sediments in the  $SREE_{CR-n}$  fractionation distribution fell between those of CR and KR sediments,

although the slope of SEYSM was steeper than that of CYSM, which had a nearly flat distribution pattern (Fig. 4). This suggests that these shelf-mud deposits are mixtures of these riverine sediments. The quantitative mixing ratios ( $k$ ) were estimated based on the difference in slopes ( $s$ ) of  $SREE_{CR-n}$  between CR and CYSM (or SEYSM), and the slope difference ( $t$ ) between CR and KR (Fig. 4):

$$K = 100 \times (s/t)$$

All relative mixing ratios of CR and KR sediments in the CYSM and SEYSM deposits are suggested in Table 2. The CYSM deposit was composed of 55–80% of the CR source in all fractions, whereas SEYSM, which developed along the southwestern coastal zone of Korea, was 10–40% of the CR source. The CR contribution to CYSM was lower in the total fractions (55% in both the silt and clay populations) than in the leached fraction (80% and 65% in silt and clay populations, respectively), probably because of the small difference in distribution patterns of the residual fraction (Fig. 4). In the leached fraction, notably, CR contributions to CYSM were higher in the silt fraction (80%) than in the clay (65%), but the contributions to SEYSM were slightly higher in the clay (40%) than the silt fraction (30%). The 40% CR contribution to SEYSM, estimated from the leached clay fraction, likely represents an upper bound, possibly due to inclusion of coarse-grained silts and sands from the nearby KRs. Likewise, the 35% KR contribution to CYSM, estimated from the leached clay fraction, can also be considered an upper bound, due to greater inclusion of coarse grains from the nearby CRs and/or Chinese coasts. This result provides tentative support for a link between the formation of CYSM deposit and KR sediments, and further reaffirms the previous studies that KR sediments can be dispersed to the central Yellow Sea as well as the Chinese coast (e.g., Jiangsu coast) (Zhao et al., 1990; Wei et al., 2003; Wang et al., 2014, Lim et al., 2015b; Li et al., 2017).

The total fraction contributed by CRs (or KRs) to CYSM and SEYSM may be underestimated because of the inclusion of the residual fraction (Table 2). The

contribution from CRs to CYSM was approximately 55% in both the silt and clay populations, which is 10–25% lower than the leached fractions. In SEYSM deposit, CR contributions were 40% and 10% in total fractions of the clay and silt populations, respectively, which were similar to the value for leached clay, but 20% lower than those for leached silt. When including the residual fraction in the total fraction as well as coarse-grained sediments from the nearby Korean Peninsula, the contribution of CR-derived silt and clay to SEYSM was estimated to be at least 40%. This estimate is higher than previous results, suggesting that ~20% of the bulk sediments were originated from the CRs (Um et al., 2015). In previous studies, qualitative CR (or KR) contributions to CYSM and SEYSM were suggested using the REE distribution pattern from the bulk sediments (e.g., Jung et al., 2012, 2016b; Lim et al., 2014, 2015b); however, these may be underestimates due to a masking effect by the residual fraction as well as the coarse-grained particles with low REE concentration.

Thus, the leached fraction in the clay populations may be appropriate for quantitatively estimating the maximum contributions of the CR or KR sediments to the Yellow Sea shelf-mud deposits, which are far away from the rivers themselves. Furthermore, our results support the presence of a CR source input to SEYSM deposits (Korean coastal regions), which is one of the most demanding and controversial issues regarding Yellow Sea source-to-sink processes (Lim et al., 2007 and references therein; Lee et al., 2020 and references therein). CR sediments account for 40% of the clay sediments in SEYSM deposits, despite its location close to the southwestern coast of Korea. This reaffirms the notion of the Korean coastal area as an important sink of CR sediments during their transportation from the south by the Yellow Sea Warm Current (Lim et al., 2007; Um et al., 2015). In addition, the CYSM deposition may be linked to KR sediments, contrary to previous results reporting that the deposit is overwhelmingly covered by sediments supplied by CRs. Although this study suggests quantitative contribution of riverine

sources to shelf-mud deposits, the dispersal pathways from rivers to these mud deposits remain elusive.

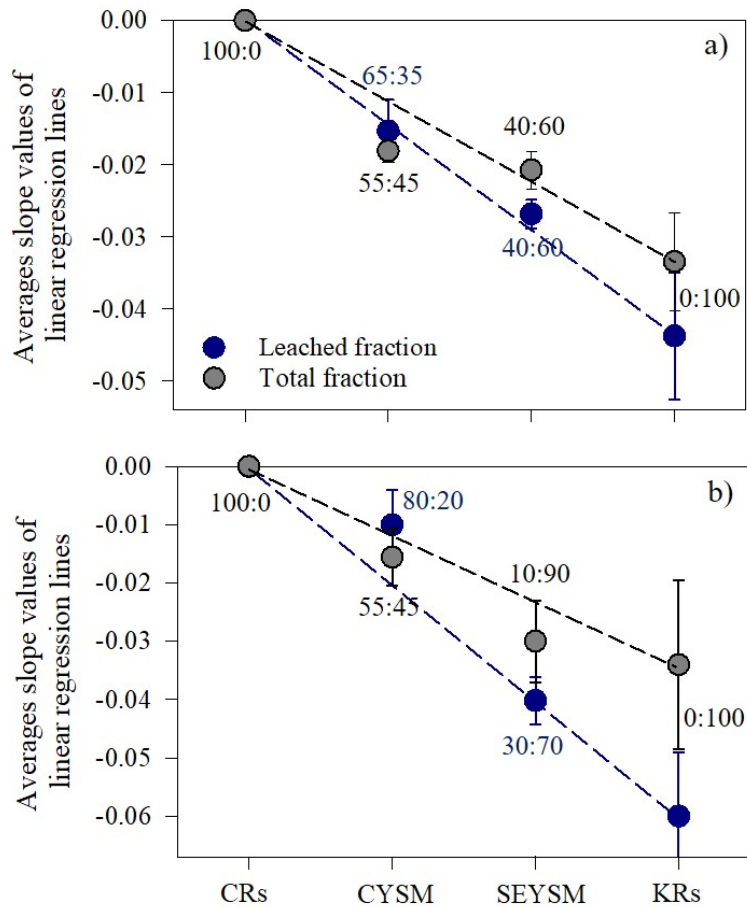


**Figure 4.** Average slope values of sediment groups in the clay (a) and silt (b) populations. Numbers indicate the sediment source mixing ratios of CRs and KRs, which are calculated based on the novel REE-source discrimination model presented in this study (see text for details). CRs: Chinese rivers, KRs: Korean rivers, CYSM: Central Yellow Sea Mud, SEYSM: Southeastern Yellow Sea Mud.

## 5. Conclusion

We proposed a new quantitative discrimination model for the Yellow Sea using the fractionation distribution characteristics of REEs. Surface sediment samples from the rivers (CRs and KRs) and shelf-mud deposits of the Yellow Sea were taken and partitioned into two grain size populations (silt and clay), and two chemical fractions (acid-leachable and residual phases). REE concentrations were analyzed for these granulometrically and chemically portioned samples, and fractionation distribution characteristics of the SREEs (i.e., REEs standardized for the GSEs) were identified and numerically indexed. Our REE-source discrimination model revealed that the shelf-mud deposits (particularly SEYSM and CYSM) are sourced from a mixture of CRs and KRs: the CRs contribute approximately 55–80% and 10–40% to CYSM and SEYSM, respectively. The leached clay fraction is considered a better material for quantitative evaluation of maximum contribution from rivers to mud deposits in the Yellow Sea and/or even in the northern East China Sea, which are far away from CRs and KRs. Notably, about 40% of the clay fraction in the southwestern Korean coastal mud deposits (i.e., SEYSM) may be derived from CRs, reaffirming that the present-day sediment discharge by KRs cannot account for the entire deposition of mud patches along the Korean coasts, suggesting an additional sediment source for the coastal mud deposits of Korea. This study provides significant insights into the dispersal system of riverine sediments in the Yellow Sea as well as the East China Sea.

**Table 2.** Quantitative contribution of CRs to the shelf mud deposits (SEYSM and CYSM) based on a new REE mixing model of two end-members presented in this study. Numbers in parentheses indicate contribution of KR.

Sediment group	Leached fraction		Total fraction	
	clay population	silt population	clay population	silt population
CRs	100 (0)	100 (0)	100 (0)	100 (0)
CYSM	65 (35)	80 (20)	55 (45)	55 (45)
SEYSM	40 (60)	30 (70)	40 (60)	10 (90)

CRs and KR: Chinese and Korean rivers, CYSM: Central Yellow Sea Mud deposits, SEYSM: Southeastern Yellow Sea Mud deposits

# Chapter 4

## Summary





Sediment provenance discrimination in the Yellow Sea and northern East China Seas (YECSs) has long been a subject of interest, but its quantification is still inconclusive. Here, we present an improved Al-Mg regression analysis by refining its methodological approach to strengthen quantitative resolution of sediment source-to-sink transports in the YECSs, with focus on its forcing mechanisms during the Holocene. Our quantitative source estimates clearly depict a considerable supply of the Chinese river (CR) sediments (~50%) to the southwestern Korean coastal region, and the Korean river (KR) sediments (30–40%) to the Central Yellow Sea Mud deposit, which accounts for a good balance between the sediment supply and budget of the shelf deposit. Of particular note is an abrupt decline in the CR contributions around 124°E, which indicates that the CR sediments do not directly reach the eastern part of the Yellow Sea blocked by a strong physical boundary. Further, the observed variations in proportions between Hunaghe-, Changjiang- and Korean river-derived sediments over the last 15 kyr – notably an abrupt increase of CR contribution since ~7 ka, followed by a sudden drop at ~3–4 ka – exhibit a good correspondence with other mineralogical proxy records. These temporal provenance changes witnessed robust palaeoenvironmental signals which fit to major climatic and oceanographic events linked with sea-level, intensity of the Kuroshio Current inflow and the East Asian monsoon. This study improves understanding of what pathways and sinks exist within the YECS basin, and how rates of sediment supply from adjacent rivers have changed over time.

Discriminating sediment sources quantitatively of several unique shelf-mud deposits in the Yellow Sea has received considerable attention, because they are active sedimentary depocenters that can elucidate the river sediment dispersal patterns and the depositional systems of the sea. Here, we propose a new sediment source proxy model of rare earth elements (REEs) that reflects innate characteristics of their fractionation distribution patterns and provides a reasonable and practical estimation for quantifying sediment source apportionments in the

Yellow Sea. REEs of riverine and shelf-mud sediments were granulometrically and chemically partitioned, and the unique characteristics of their fractionation patterns were recorded and numerically indexed. We found distinct differences in the REE fractionation pattern index of riverine sediments, possibly due to the different source rock compositions. Notably, the acid-leached phase of the clay fraction may be a better material for quantitative evaluation of river contributions in the Yellow Sea. Using the REE-source index model presented here, proportional contributions of Chinese river sediments to the central and southeastern Yellow Sea mud deposits were estimated to be 55–80% and 10–40%, respectively, with higher percentage in the leached fraction. Our results elucidate the disagreement between mud budget and river discharge, particularly in Korean coastal mud deposits, as well as the source interpretation of the Yellow Sea shelf-mud deposits, which have been debated since the 1980s.

Conclusively, marine sediment-provenance changes are closely linked to marine-terrestrial climatic changes, and therefore information on their historical variations can play a crucial role in projecting future state of land-ocean interactions driven by global warming. Further, the establishment of sediment-provenance quantification provides high-level policy advice to governments with scientific strategies in terms of national and international marine management issues (e.g., changes in marine environments, ecosystems and resources thereof, marine pollution and maritime boundary delimitation).

(The contents of this research report are published in two international journals (Marine Geology and Continental Shelf Research). The sediment samples for this work were provided by the Library of Marine Samples (LIMS) of Korea Institute of Ocean Science & Technology, Korea).

# Chapter 5



## References

- Alexander, C.R., DeMaster, D.J., Nittrouer, C.A., 1991. Sediment accumulation in a modern epicontinental-shelf setting: The Yellow Sea. *Mar. Geol.* 98, 51–72.
- Babechuk, M.G., Widdowson, M., Kamber, B.S., 2014. Quantifying chemical weathering intensity and trace element release from two contrasting basalt profiles, Deccan Traps, India. *Chem. Geol.* 363, 56–75.
- Bian, C., Jiang, W., Greatbatch, R.J., 2013. An exploratory model study of sediment transport sources and deposits in the Bohai Sea, Yellow Sea, and East China Sea. *J. Geophys. Res. Oceans* 118, 5908–5923, doi:10.1002/2013JC009116.
- Bian, C., Jiang, W., Song, D., 2010. Terrigenous transportation to the Okinawa Trough and the influence of typhoons on suspended sediment concentration. *Cont. Shelf Res.* 30, 1189–1199.
- Chang, T.S., Ha, H.J., 2015. The Heuksan mud belt on the tide-dominated shelf of Korea: a supply-driven depositional system? *Geo-Mar. Lett.* 35, 447–460.
- Chen, C.-T. A., 2009. Chemical and physical fronts in the Bohai, Yellow and East China seas. *J. Mar. Sys.* 78, 394–410.
- Cho, H.G., Kim, S.O., Kwak, K.Y., Choi, H.S., Kim, B.K., 2015. Clay mineral distribution and provenance in the Heuksan mud belt, Yellow Sea. *Geo-Mar. Lett.* 35, 411–419.
- Cho, Y.G., Lee, C.B., Choi, M.S., 1999. Geochemistry of surface sediments off the southern and western coast of Korea. *Mar. Geol.* 159, 111–129.
- Chough, S.K., Kim, J.W., Lee, S.H., Shinn, Y.J., Jin, J.H., Suh, M.C., Lee, J.S., 2002. High-resolution acoustic characteristics of epicontinental sea deposits, central-eastern Yellow Sea. *Mar. Geol.* 188, 317–331.
- Cronan, D.S., Hodkinson, R.A., 1997. Geochemistry of hydrothermal sediments from ODP Sites 834 and 835 in the Lau Basin, southwest Pacific. *Mar. Geol.* 141, 237–268.
- Cullers, R.L., Graf, J., 1983. Rare earth elements in igneous rocks of the continental crust: intermediate and silicic rocks, ore petrogenesis. In: Henderson, P. (Ed.), *Rare Earth Element Geochemistry*. Elsevier, Amsterdam, pp. 275–312.
- Dinis, P., Garzanti, E., Vermeesch, P., Huvi, J., 2017. Climatic zonation and weathering control on sediment composition (Angola). *Chem. Geol.* 467, 110–121.

- Dong, L.X., Guan, W.B., Chen, Q., Li, X.H., Liu, X.H., Zeng, X.M., 2011. Sediment transport in the Yellow Sea and East China Sea. *Estuar. Coast. Shelf Sci.* 93, 248–258.
- Dou, Y.G., Yang, S.Y., Lim, D.I., Jung, H.S., 2015. Provenance discrimination of last deglacial and Holocene sediments in the southwest of Cheju Island, East China Sea. *Palaeogeogr. Palaeoclimatol. Palaeoecol.* 422, 25–35.
- Feng, J., Hua, Z-G., Ju, J-T., Zhu, L-P., 2011. Variations in trace element (including rare earth element) concentrations with grain sizes in loess and their implications for tracing the provenance of eolian deposits. *Quat. Int.* 236, 116–126.
- Gao, S., Collins, M.B., 2014. Holocene sedimentary systems on continental shelves. *Mar. Geol.* 352, 268–294.
- Gao, S., Wang, D., Yang, Y., Zhou, L., Zhao, Y., Gao, W., Han, Z., Yu, Q., Li, G., 2015. Holocene sedimentary systems on a broad continental shelf with abundant river input: process–product relationships. In: Clift, P.D., Harff, J., Wu, J., Yan, Q. (Eds.), *River-dominated shelf sediments of East Asian Seas*. Geological Society, London, Special publications, pp. 1–37. <http://doi.org/10.1144/SP429.4>.
- Hickox, R., Belkin, I., Cornillon, P., Shan, Z., 2000. Climatology and seasonal variability of ocean fronts in the East China, Yellow and Bohai seas from satellite SST data. *Geophys. Res. Lett.* 27(18), 2945–2948.
- Hori, K., Saito, Y., Zhao, Q., Cheng, X., Wang, P., Sato, Y., Li, C., 2001. Sedimentary facies and Holocene progradation rates of the Changjiang (Yangtze) delta, China. *Geomorphology* 41, 233–248.
- Hu, B.Q., Li, G., Li, J., Yang, M., Wang, L., Bu, R., 2011. Spatial variability of the <sup>210</sup>Pb sedimentation rates in the Bohai and Huanghai Seas and its influencing factors. *Acta Oceanol. Sin.* 33, 125–133.
- Hu, B.Q., Yang, Z.S., Qiao, S.Q., Zhao, M.X., Fan, D.J., Wang, H.J., Bi, N.S., Li, J., 2014. Holocene shifts in riverine fine-grained sediment supply to the East China Sea Distal Mud in response to climate change. *The Holocene* 24, 1253–1268.
- Hu, D.X., 1984. Upwelling and sedimentation dynamics. *J. Chinese Oceanol. Limnol.* 1984, 12–19.

- Hu, D.X., Li, Y.X., 1993. Study of ocean circulation. In: Tseng, C.K., Zhou, H.O., Li, B.C. (Eds.), *Marine science study and its prospect in China*. Qingdao Publishing House, pp. 513–516.
- Huang, J., Wan, S., Xiong, Z., Zhao, D., Liu, X., Li, A., Li, T., 2016. Geochemical records of Taiwan-sourced sediments in the South China Sea linked to Holocene climate changes. *Palaeogeogr. Palaeoclimatol. Palaeoecol.* 441(4), 871-881.
- Jian, Z., Wang, P., Saito, Y., Wang, J., Pflaumann, U., Oba, T., Cheng, X., 2000. Holocene variability of the Kuroshio current in the Okinawa Trough, northwestern Pacific Ocean. *Earth Planet. Sci. Lett.* 184, 305–319.
- Jung, H.S., Lim, D.I., Choi, J.Y., Yoo, H.S., Rho, K.C., Lee, H.B., 2012. Rare earth element compositions of core sediments from the shelf of the South Sea, Korea: Their controls and origins. *Cont. Shelf Res.* 48, 75–86.
- Jung, H.S., Lim, D.I., Xu, Z.K., Jeong, K.S., 2016a. Secondary grain-size effects on Li and Cs concentrations and appropriate normalization procedures for coastal sediments. *Estuar. Coast. Shelf Sci.* 20, 57–61.
- Jung, H.S., Lim, D.I., Jeong, D.H., Xu, Z.K., Li, T., 2016b. Discrimination of sediment provenance in the Yellow Sea: Secondary grain-size effect and REE proxy. *J. Asian Earth Sci.* 123, 78–84.
- Jung, H.S., Lim, D.I., Xu, Z.K., Kang, J.H., 2014. Quantitative compensation of grain-size effects in elemental concentration: a Korean coastal sediments case study. *Estuar. Coast. Shelf Sci.* 151, 69–77.
- Jung, H.S., Lim, D.I., Yang, S.Y., Yoo, H.S., 2006. Constraints of REE distribution patterns in core sediments and their provenance, northern East China Sea. *Economic and Environ. Geol.* 39, 39-51. In Korean with English abstract.
- Kajita, H., Kawahata, H., Wang, K., Zheng, H., Yang, S., Ohkouchi, N., Utsunomiya, M., Zhou, B., Zheng, B., 2018. Extraordinary cold episodes during the mid-Holocene in the Yangtze delta: interruption of the earliest rice cultivating civilization. *Quat. Sci. Rev.* 201, 418–428.
- KIGAM, 1996. Yellow Sea drilling program for studies on Quaternary geology. KIGAM Research Report KR-96(T)-18, Daejeon, Korea. p. 595.
- Kim, G.B., Yang, H.S., Church, T.M., 1999. Geochemistry of alkaline earth elements (Mg, Ca, Sr, Ba) in the surface sediments of the Yellow Sea. *Chemical*

Geology 153, 1–10.

- Kim, S.Y., Lim, D.I., 2014. Signatures of the late Holocene Neoglacial cold event their marine-terrestrial linkage in the northwestern Pacific margin. *Prog. Oceanogr.* 124, 54–65.
- Kong, G.S., Park, S.C., Han, H.C., Chang, J.H., Mackensen, A., 2006. Late Quaternary paleoenvironmental changes in the southeastern Yellow Sea, Korea. *Quat. Int.* 144, 38–52.
- Koo, H.J., Lee, Y.J., Kim, S.O., Cho, H.G., 2018. Clay mineral distribution and provenance in surface sediments of Central Yellow Sea Mud. *Geosci. J.* 22, 989–1000.
- Lee, C.B., Jung, H.S., Jeong, K.S., 1992. Distribution of some metallic elements in surface sediments of the southeastern Yellow Sea. *J. Korean Soc. Oceanogr.* 27, 55–65.
- Lee, G.S., Kim, D.C., Yoo, D.G., Yi, H.I., 2014. Stratigraphy of late Quaternary deposits using high resolution seismic profile in the southeastern Yellow Sea. *Quat. Int.* 344, 109–124.
- Lee, G.S., Yoo, D.G., Bae, S.H., Min, G.H., Kim, S.P., Choi, H., 2015. Seismic stratigraphy of the Heuksan mud belt in the southeastern Yellow Sea, Korea. *Geo-Mar. Lett.* 35:433–446.
- Lee, H.J., 2015. A review on the Holocene evolution of an inner-shelf mud deposit in the southeastern Yellow Sea: the Huksan Mud Belt. *Geo-Mar. Lett.* 50, 615–621.
- Lee, H.J., Chough, S.K., 1989. Sediment distribution, dispersal and budget in the Yellow Sea. *Mar. Geol.* 87, 195–205.
- Lee, H.J., Chu, Y.S., 2001. Origin of inner-shelf mud deposit in the southeastern Yellow Sea: Huksan Mud Belt. *J. Sediment. Res.* 71, 144–154.
- Lee, H.J., Jeon, C.K., Lim, H.S., 2020. Dynamic analysis of the mud-belt formation in the Bohai, Yellow and East China Seas. *Mar. Geol.* 423, 106–140.
- Lee, H.J., Jeong, K.S., Han, S.J., Bahk, K.S., 1988. Heavy minerals indicative of Holocene transgression in the southeastern Yellow Sea. *Cont. Shelf Res.* 8, 255–266.
- Li, G.X., Li, P., Liu, Y., Qiao, L.L., Ma, Y.Y., Xu, J.S., Yang, Z.G., 2014a. Sedimentary system response to the global sea level change in the East China

- Seas since the last glacial maximum. *Earth-Sci. Rev.* 139, 390–405.
- Li, G.X., Qiao, L., Dong, P., Ma, Y., Xu, J., Liu, S., Liu, Y., Li, J., Li, P., Ding, D., Wang, N., A., D.O., Liu, L., 2016a. Hydrodynamic condition and suspended sediment diffusion in the Yellow Sea and East China Sea. *J. Geophys. Res. Oceans* 121, 6204–6222. doi:10.1002/2015JC011442.
- Li, J., Hu, B., Wei, H., Zhao, J., Zou, L., Bai, F., Dou, Y., Wang, L., Fang, X., 2014b. Provenance variations in the Holocene deposits from the southern Yellow Sea: Clay mineralogy evidence. *Cont. Shelf Res.* 90, 41–51.
- Li, L., Su, J.B., Rao, W.B., Wang, Y.G., 2017. Using geochemistry of rare earth elements to indicate sediment provenance of sand ridges in southwestern Yellow Sea. *Chinese Geogra. Sci.* 27, 63–77.
- Li, W., Wang, Z., Huang, H., 2019. Relationship between the southern Yellow Sea Cold Water Mass and the distribution and composition of suspended particulate matter in summer and autumn seasons. *J. Sea Res.* 154, 101812.
- Li, X.S., Zhao, Y.X., Feng, Z.B., Liu, C.G., Xie, Q.H., Zhou, Q.J., 2016b. Quaternary seismic facies of the south Yellow Sea shelf: depositional processes influenced by sea-level change and tectonic controls. *Geol. J.* 51, 77–95.
- Lie, H.J., 1989. Tidal fronts in the southeastern Hwanghae (Yellow Sea). *Cont. Shelf Res.* 9, 527–546.
- Lie, H.J., Cho, C.H., Lee, J.H., Lee, S., 2003. Structure and eastward extension of the Changjiang River plume in the East China Sea. *J. Geophys. Res. Oceans* 108, 3077.
- Lim, D.I., Choi, J.Y., Jung, H.S., Rho, K.C., Ahn, K.S., 2007. Recent sediment accumulation and origin of shelf mud deposits in the Yellow and East China Seas. *Prog. Oceanogr.* 73, 145–159.
- Lim, D.I., Choi, J.Y., Shin, H.H., Rho, K.C., Jung, H.S., 2013. Multielement geochemistry of offshore sediment origin and dispersal. *Quatern. Int.* 298, 196–206.
- Lim, D.I., Jung, H.S., Choi, J.Y., 2014. REE partitioning in riverine sediments around the Yellow Sea and its importance in shelf sediment provenance. *Mar. Geol.* 357, 12–24.
- Lim, D.I., Jung, H.S., Choi, J.Y., Yang, S., Ahn, K.S., 2006. Geochemical compositions of river and shelf sediments in the Yellow Sea: grain-size



- normalization and sediment provenance. *Cont. Shelf Res.* 26, 15–24.
- Lim, D.I., Jung, H.S., Xu, Z., Jeong, K.S., Li, T., 2015a. Elemental and Sr-Nd isotopic compositional disparity of riverine sediments around the Yellow Sea: Constraints from grain-size and chemical partitioning. *Appl. Geochem.* 63, 272–281.
- Lim, D.I., Kim, J.H., Xu, Z.K., Jeong, K.S., Jung, H.S., 2017. New evidence for Kuroshio inflow and deepwater circulation in the Okinawa Trough, East China Sea: sedimentary mercury variations over the last 20 kyr. *Paleoceanography* 32, 571–579.
- Lim, D.I., Xu, Z., Choi, J.Y., Li, T., Kim, S.Y., 2015b. Holocene changes in detrital sediment supply to the eastern part of the central Yellow Sea and their forcing mechanisms. *J. Asian Earth Sci.* 105, 18–31.
- Lim, J.S., Matsumoto, E., 2008. Fine aeolian quartz records in Cheju Island, Korea, during the last 6500 years and pathway change of the westerlies over east Asia. *J. Geophys. Res.* 113, D08106.
- Lim, J.S., Matsumoto, E., Kitagawa, H., 2005. Eolian quartz flux variations in Cheju Island, Korea during the last 6500 yr and a possible Sun-monsoon linkage. *Quat. Res.* 64, 12–20.
- Liu, J.P., Xu, K.H., Li, A.C., Milliman, J.D., Velozzi, D.M., Xiao, S.B., Yang, Z.S., 2007. Flux and fate of Yangtze River sediment delivered to the East China Sea. *Geomorphology* 85, 208–224.
- Mascarenhas-Pereira, M.B.L., Nath, B.N., 2010. Selective leaching studies of sediments from a seamount flank in the Central Indian Basin: resolving hydrothermal, volcanogenic and terrigenous components using major, trace and rare-earth elements. *Mar. Chem.* 121, 49–66.
- McLennan, S.M., 1989. Rare earth elements in sedimentary rocks; influence of provenance and sedimentary processes. In: Ripin, B.R. and McKay, G.A. (Eds.), *Reviews in Mineralogy and Geochemistry*, vol. 21 (Geochemistry and Mineralogy of Rare Earth Elements), Mineral Society of America, pp.169–200.
- Milliman, J.D., Li, F., Zhao, Y.Y., Zheng, T.M., 1986. Suspended matter regime in the Yellow Sea. *Prog. Oceanogr.* 17, 215–227.
- Milliman, J.D., Meade, R.H., 1983. World-wide delivery of river sediment to the oceans. *J. Geol.* 91, 1–21.

- Milliman, J.D., Qin, Y.S., Ren, M.E., Saito, Y., 1987. Man's influence on the erosion and transport of sediment by Asian rivers: The Yellow River (Huanghe) example. *The J. Geol.* 95, 751–762.
- Milliman, J.D., Shen, H.T., Yang, Z.S., Meade, R.H., 1985. Transport and deposition of river sediment in the Changjiang estuary and adjacent continental shelf. *Cont. Shelf Res.* 4, 37–45.
- Moon, J., Pang, I., Yoon, J., 2009. Response of the Changjiang diluted water around Jeju Island to external forcings: a modeling study of 2002 and 2006. *Cont. Shelf Res.* 29, 1549–1564.
- Naimie, C.E., Blain, C.A., Lynch, D.R., 2001. Seasonal mean circulation in the Yellow Sea—a model-generated climatology. *Cont. Shelf Res.* 21, 667–695.
- Nesbitt, H.W., Markovics, G., Price, R.C., 1980. Chemical process affecting alkalis and alkaline earths during continental weathering. *Geochim. Cosmochim. Acta* 44, 1659–1666.
- Nyakairu, G.W.A., Koeberl, C., 2001. Mineralogical and chemical composition and distribution of rare earth elements in clay-rich sediments from central Uganda. *Geochem. J.* 35, 13–28.
- Palmer, M.R., 1985. Rare earth elements in foraminifera tests. *Earth Planet. Sci. Lett.* 73, 285–298.
- Park, S.C., Lee, H.H., Han, H.S., Lee, G.H., Kim, D.C., Yoo, D.G., 2000. Evolution of late Quaternary mud deposits and recent sediment budget in the southeastern Yellow Sea. *Mar. Geol.* 170, 271–288.
- Park, J., Park, J., Yi, S., Kim, J.C., Lee, E., Choi, J., 2019. Abrupt Holocene climate shifts in coastal East Asia, including the 8.2 ka, 4.2 ka, and 2.8 ka BP events, and societal response on the Korean peninsula. *Sci. Rep.* 9, 10806.
- Park, Y.A., Khim, B.K., 1992. Origin and dispersal of recent clay minerals in the Yellow Sea. *Mar. Geol.* 104, 205–213.
- Prego, R., Caetano, M., Vale, C., Marmolejo-Rodriguez, J., 2009. Rare earth elements in sediments of the Vigo Ria, NW Iberian Peninsula. *Cont. Shelf Res.* 29, 896–902.
- Qiao, S., Shi, X., Wang, G., Zhou, L., Hu, B., Hu, L., Yang, G., Liu, Y., Yao, Z., Liu, S., 2017. Sediment accumulation and budget in the Bohai Sea, Yellow

- Sea and East China Sea. *Mar. Geol.* 390, 270–281.
- Rao, W.B., Mao, C.P., Wang, Y.G., Su, J.B., Balsam, W., Ji, J.F., 2015. Geochemical constraints on the provenance of surface sediments of radial sand ridges off the Jiangsu coastal zone, East China. *Mar. Geol.* 359, 35–49.
- Ren, M.E., Shi, Y.L., 1986. Sediment discharge of the Yellow River (China) and its effect on the sedimentation of the Bohai and the Yellow Sea. *Cont. Shelf Res.* 6, 785–810.
- Ren, M.E., Zhu, X., 1994. Anthropogenic influences on changes in the sediment load of the Yellow River, China, during the Holocene. *The Holocene* 4, 314–320.
- Ren, S., Xie, J., Zhu, S., 2014. The roles of different mechanisms related to the tide-induced fronts in the Yellow Sea in summer. *Adv. Atmos. Sci.* 31, 1079–1089.
- Ruttenberg, K.C., Goñi, M.A., 1997. Phosphorus distribution, C:N:P ratios, and  $\delta^{13}\text{C}_{\text{oc}}$  in arctic, temperate, and tropical coastal sediments: tools for characterizing bulk sedimentary organic matter. *Mar. Geol.* 139, 123–145.
- Saito, Y., Katayama, H., Ikehara, K., 1998. Transgressive and highstand systems tracts and post-glacial transgression, the East China Sea. *Sediment. Geol.* 122, 217–232.
- Sanematsu, K., Murakami, H., Watanabe, Y., Duangsurigna, S., Vilayhack, S., 2009. Enrichment of rare earth elements (REE) in granitic rocks and their weathered crusts in central and southern Laos. *Bull. Geol. Sur. Japan* 60, 527–558.
- Shi, X.F., Shen, S.X., Yi, H.I., Chen, Z.H., Meng, Y., 2003. Modern sedimentary environments and dynamic depositional systems in the southern Yellow Sea. *Chin. Sci. Bull.* 48, 1–7.
- Sholkovitz, E.R., 1990. Rare-earth elements in marine sediments and geochemical standards. *Chem. Geol.* 88, 333–347.
- Singh, P., Rajamani, V., 2001. REE geochemistry of recent clastic sediments from the Kaveri floodplains, southern India: implication to source area weathering and sedimentary processes. *Geochim. Cosmochim. Acta* 65, 3093–3108.
- Song, Y.H., Choi, M.S., 2009. REE geochemistry of fine-grained sediments from major rivers around the Yellow Sea. *Chem. Geol.* 266, 328–342.
- Stein, R., 1991. Accumulation of organic carbon in marine sediments. Results from the deep sea drilling project/ocean drilling program. In: Bhattacharji, S.,

- Friedman, G.M., Neugebauer, H.J., Seilacher, A. (Eds.), *Lecture notes in earth sciences*, Berlin, 34, 30–31.
- Su, N., Yang, S., Guo, W., Yue, W., Wang, X., Yin P., Huang, X., 2017. Revisit of rare earth element fractionation during chemical weathering and river sediment transport. *Geochem. Geophys. Geosyst.* 18, 935–955.
- Uehara, K., Saito, Y., 2003. Late Quaternary evolution of the Yellow/East China Sea tidal regime and its impacts on sediments dispersal and sea floor morphology. *Sediment. Geol.* 162, 25–38.
- Um, I.K., Choi, M.S., Lee, G.S., Chang, T.S., 2015. Origin and depositional environment of fine-grained sediments since the last glacial maximum in the southeastern Yellow Sea: evidence from rare earth elements. *Geo-Mar. Lett.* 35, 421–431.
- Wang, H., Yang, Z., Saito, Y., Liu, J., Sun, X., Wang, Y., 2007. Stepwise decreases of the Huanghe (Yellow River) sediment load (1950–2005): Impacts of climate change and human activities. *Global Planet. Change* 57, 331–354.
- Wang, L., Li, G., Xu, J., Liu, Y., Qiao, L., Ding, D., Yang, J., Dada, Q.A., Li, Q., 2019. Strata sequence and paleochannel response to tectonic, sea-level, and Asian monsoon variability since the late Pleistocene in the South Yellow Sea. *Quat. Res.* 1–19.
- Wang, L.J., Li, X.X., Zhang, S., Zhang, C.S., 1994. A study on the contents and speciation of rare earth elements in the water body in the Wuhan section of the Yangtze River. *Acta Geogr. Sin.* 49, 353–362.
- Wang, Q., Yang, S.Y., 2013. Clay mineralogy indicates the Holocene monsoon climate in the Changjiang (Yangtze River) Catchment, China. *Appl. Clay Sci.* 74, 28–36.
- Wang, Y., Li, G., Zhang, W., Dong, P., 2014. Sedimentary environment and formation mechanism of the mud deposit in the central South Yellow Sea during the past 40 ky. *Mar. Geol.* 347, 123–135.
- Wang, Z., Chen, Z., Tao, J., 2006. Clay mineral analysis of Yangtze delta, China, to interpret the late Quaternary sea-level fluctuations, climate change and sediment provenance. *J. Coast. Res.* 22(3), 683–691.
- Wang, Z., Li, M., Zhang, R., Zhuang, C., Liu, Y., Saito, Y., Xie, J., Zhao, B., 2011. Impacts of human activity on the late-Holocene development of the

- subaqueous Yangtze delta, China, as shown by magnetic properties and sediment accumulation rates. *The Holocene* 21, 393–407.
- Wang, Z.B., Yang, S.Y., Li, R.H., Zhang, Z.X., Li, J., Bai, F.L., Li, C., 2010. Detrital mineral composition of the sediments from Huanghe and its hydrodynamic. *Mar. Geol. Quat. Geol.* 30, 73–85. In Chinese with English abstract.
- Wei, J.W., Shi, X.F., Li, G.X., Liang, R.C., 2003. Clay mineral distributions in the southern Yellow Sea and their significance. *Chin. Sci. Bull.* 48, 7–11.
- Xiang, R., Sun, Y.B., Li, T.G., Oppo, D.W., Chen, M.H., Zheng, F., 2007. Paleoenvironmental change in the middle Okinawa Trough since the last deglaciation: evidence from the sedimentation rate and planktonic foraminiferal record. *Palaeogeogr. Palaeoclimatol. Palaeoecol.* 243, 378–393.
- Xiang, R., Yang, Z.S., Saito, Y., Guo, Z.G., Fan, D.J., Li, Y.H., Xiao, S.B., Shi, X., Chen, M.H., 2006. East Asia Winter Monsoon changes inferred from environmentally sensitive grain size component records during the last 2500 years in mud area southwest off Cheju Island, ECS. *Sci. China Ser. D* 49(6), 604–614.
- Xu, Z., Lim, D.I., Li, T., Kim, S.Y., Jung, H.S., Wan, S., Chang, F., Cai, M., 2019. REEs and Sr-Nd isotope variations in a 20 ky-sediment core from the middle Okinawa Trough, East China Sea: An in-depth provenance analysis of siliciclastic components. *Mar. Geol.* 415, 105970.
- Xu, Z.K., Lim, D.I., Choi, J.Y., Yang, S.Y., Jung, H.S., 2009. Rare earth elements in bottom sediments of major rivers around the Yellow Sea: implications for sediment provenance. *Geo-Mar. Lett.* 29, 291–300.
- Yang, H.W., Cho, Y.K., Seo, G.H., You, S.H., Seo, J.W., 2014a. Interannual variation of the southern limit in the Yellow Sea Bottom Cold Water and its causes. *J. Mar. Syst.* 139, 119–127.
- Yang, S.Y., Jung, H.S., Choi, M.S., Li, C.X., 2002. The rare earth element compositions of the Changjiang (Yangtze) and Huanghe (Yellow) river sediments. *Earth Planet. Sci. Lett.* 201, 407–419.
- Yang, S.Y., Jung, H.S., Li, C.X., 2004. Two unique weathering regimes in the Changjiang and Huanghe drainage basins: geochemical evidence from river sediments. *Sediment. Geol.* 164, 19–34.
- Yang, S.Y., Jung, H.S., Lim, D.I., Li, C.X., 2003a. A review on the provenance

- discrimination of sediments in the Yellow Sea. *Earth-Sci. Rev.* 63, 93–120.
- Yang, S.Y., Li, C.X., Lee, C.B., Na, T.K., 2003b. REE geochemistry of suspended sediments from the rivers around the Yellow Sea and provenance indicators. *Chinese Sci. Bull.* 48, 1135–1139.
- Yang, S.Y., Lim, D.I., Jung, H.S., Oh, B.C., 2004. Geochemical composition and provenance discrimination of coastal sediments around Cheju Island in the southeastern Yellow Sea. *Mar. Geol.* 206, 41–53.
- Yang S.Y., Wang, Z.B., Dou, Y.G., Shi., X.F., 2014b. A review of sedimentation since the last glacial maximum on the continental shelf of eastern China. In: Chiocci, F.L., Chivas, A.R. (Eds.), *Continental shelves during last glacio-eustatic cycle: shelves of the world*. Geological Society, London, *Memoirs*, 41, 293–303. [https:// doi:10.1144/M41.21](https://doi.org/10.1144/M41.21).
- Yang, S.Y., Youn, J.S., 2007. Geochemical compositions and provenance discrimination of the central Yellow Sea sediment. *Mar. Geol.* 243, 229–241.
- Yang, Z.S., Guo, Z., Wang, Z., Xu, J., Gao, W., 1992. Basic pattern of transport of suspended matter from the Yellow Sea and East China Sea to the eastern deep seas. *Acta Oceanol. Sin.* 14, 81–90. (in Chinese).
- Yang, Z.S., Liu, J.P., 2007. A unique Yellow River-derived distal subaqueous delta in the Yellow Sea. *Mar. Geol.* 240, 169–176.
- Yoo, D.G., Lee, C.W., Kim, S.P., Jin, J.H., Kim, J.K., Han, H.C., 2002. Late Quaternary transgressive and highstand systems tracks in the northern East China Sea mid-shelf. *Mar. Geol.* 187, 313–328.
- Youn, J.S., Kim, T.J., 2011. Geochemical composition and provenance of muddy shelf deposits in the East China Sea. *Quat. Int.* 230, 3–12.
- Yu, S., Yao, P., Liu, J. Zhao, B., Zhang, G., Zhao, M., Yu, Z., Zhang, Z-H., 2016. Diversity, abundance, and niche differentiation of ammonia-oxidizing prokaryotes in mud deposits of the eastern China marginal seas. *Front. Microbiol.* 7, 137.
- Yuan, D.L., Zhu, J.R., Li, C.Y., Hu, D.X., 2008. Cross-shelf circulation in the Yellow and East China Seas indicated by MODIS satellite observations. *J. Mar. Syst.* 70, 134–149.
- Zeng, X., He, R., Xue, Z., Wang, H., Wang, Y., Yao, Z., Guan, W., Warrillow, J., 2015. River-derived sediment suspension and transport in the Bohai, Yellow,

- and East China Seas: a preliminary modeling study. *Cont. Shelf Res.* 111, 112–125.
- Zhang, C., Wang, L., Zhang, S., 1998. Geochemistry of rare earth elements in the mainstream of the Yangtze River, China. *Appl. Geochem.* 13, 451–462.
- Zhang, J., 1999. Heavy metal compositions of suspended sediments in the Changjiang estuary: significance of riverine transport to the ocean. *Cont. Shelf Res.* 19, 1521–1543.
- Zhang, K., Li, A., Huang, P., Lu, J., Liu, X., Zhang, J., 2019. Sedimentary responses to the cross-shelf transport of terrigenous material on the East China Sea Continental Shelf. *Sediment. Geol.* 384, 50–59.
- Zhang, X., Zhang, F., Chen X., Zhang, W., Deng H., 2012. REEs fractionation and sedimentary implication in surface sediments from eastern South China Sea. *J. Rare Earths* 30, 614–620.
- Zhang, Y., Gao, X., 2015. Rare earth elements in surface sediments of a marine coast under heavy anthropogenic influence: The Bohai Bay, China. *Estuar. Coast. Shelf Sci.* 164, 86–93.
- Zhao, Y.Y., Park, Y.A., Qin, Y.S., Gao, S., Zhang, F.G., Yu, J.J., 1997. Recent development in the southern Yellow Sea sedimentology: China–Korea joint investigation. *Yellow Sea* 3, 47–51.
- Zhao, Y.Y., Qin, Z.Y., Li, F.Y., Chen, Y.W., 1990. On the source and genesis of the mud in the central area of the south Yellow Sea. *Chin. J. Oceanol. Limn.* 8, 66–73.
- Zhou, C., Dong, P., Li, G., 2015. Hydrodynamic processes and their impacts on the mud deposit in the southern Yellow Sea. *Mar. Geol.* 360, 1–16.
- Zhou, L., Liu, J., Saito, Y., Zhang, Z., Chu, H., Hu, G., 2014. Coastal erosion as a major sediment supplier to continental shelves: Example from the abandoned Old Huanghe (Yellow River) delta. *Cont. Shelf Res.* 82, 43–59.
- Zhu, J., Shi, J., Guo, X., Gao, H., Yao, X., 2018. Air-sea heat flux control on the Yellow Sea Cold Water Mass intensity and implications for its prediction. *Cont. Shelf Res.* 152, 14–26.

# Chapter 6

## Appendix





# 황해-(북)동중국해 대륙붕 퇴적물의 기원지(S2S) 정량화 연구

## Quantification of sediment **source-to-sink (S2S)** in the Yellow and northern East China Sea shelves

Keywords: sediment source, quantification, EEZ, Yellow-East China Seas

2020. 11

책임연구원 임동일

### 1. 연구의 필요성 (중요성)

#### Previous study of S2S in the YECSSs

##### Source discrimination proxy

- River source end-members
- Simple proxy: spatial distribution of smectite and elemental compositions

##### Review of provenance study (~100 papers)

- Controversial issues (proxies, interpretation)
- Multi-source theory of mud deposits
- Sediment budgets & transport pathway

● 1990's Beginning stage

● 2000's Take-off stage

2006 KC joint conference  
(Turning point)

##### Quantification of S2S

● Recent

● 2010's Development stage

##### Source to sink (S2S) study / Qualitative Analysis

- Diversification of proxies (REEs, isotopes)
- Dispersal patterns of sediments
- Elemental ratios (Ee/Al)



Available online at  
SCIENCE  
Earth-Science Reviews 63 (2012) 1–12  
www.elsevier.com/locate/earscres

A review on the provenance discrimination of sediments  
in the Yellow Sea

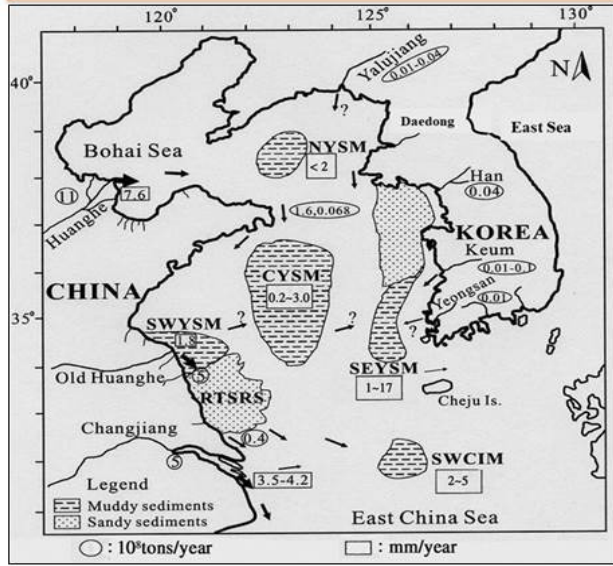
Shou Ye Yang<sup>a,b,\*</sup>, Hoi Soo Jung<sup>b</sup>, Dong Il Lim<sup>b</sup>, Cong Xian Li<sup>a</sup>

<sup>a</sup>Laboratory of Marine Geology, Tsinghua University, Shanghai 200082, China  
<sup>b</sup>Marine Environment and Climate Change Laboratory, Korea Ocean Research and Development Institute, Ansan P.O. Box 29,  
Sanae 425-600, South Korea  
Received 24 January 2010; accepted 7 February 2011

[S2S research papers: 22 편]

<p><b>Marine Geology</b></p> <p>REE partitioning in riverine sediments around the Yellow Sea and its importance in shelf sediment provenance</p> <p>Dhongi Lim<sup>a,*</sup>, Hui Soo Jung<sup>b</sup>, Jin Yong Choi<sup>c</sup></p>	<p><b>Continental Shelf Research</b></p> <p>Geochemical compositions of river and shelf sediments in the Yellow Sea: Grain-size normalization and sediment provenance</p> <p>D.I. Lim<sup>a,*</sup>, H.S. Jung<sup>b</sup>, J.Y. Choi<sup>c</sup>, S. Yang<sup>d</sup>, K.S. Ahn<sup>e</sup></p>	<p><b>Progress in Oceanography</b></p> <p>Recent sediment accumulation and origin of shelf mud deposits in the Yellow and East China Seas</p> <p>D.I. Lim<sup>a,*</sup>, J.Y. Choi<sup>b</sup>, H.S. Jung<sup>c</sup>, K.C. Rho<sup>d</sup>, K.S. Ahn<sup>e</sup></p>
<p><b>Continental Shelf Research</b></p> <p>Rare earth element compositions of core sediments from the shelf of the South Sea, Korea: Their controls and origins</p> <p>Hui-Soo Jung<sup>a</sup>, Dhongil Lim<sup>b,*</sup>, Jin-Yong Choi<sup>c</sup>, Hae-Soo Yoo<sup>d</sup>, Kyung-Chan Rho<sup>e</sup>, Hyun-Bok Lee<sup>f</sup></p>	<p><b>Quaternary International</b></p> <p>Multielement geochemistry of offshore sediments in the southeastern Yellow Sea and implications for sediment origin and dispersal</p> <p>Dhongi Lim<sup>a</sup>, Jin Yong Choi<sup>b</sup>, Hyun Bok Shin<sup>c</sup>, Kyung Chan Rho<sup>d</sup>, Hui Soo Jung<sup>e,*</sup></p>	<p><b>Applied Geochemistry</b></p> <p>Elemental and Sr-Nd isotopic compositional disparity of riverine sediments around the Yellow Sea: Constraints from grain-size and chemical partitioning</p> <p>Dhongi Lim<sup>a,*</sup>, Hui-soo Jung<sup>b</sup>, Zhaokai Xu<sup>c,*</sup>, Kapsook Jeong<sup>d</sup>, Tiegang Li<sup>e</sup></p>
<p><b>Journal of Asian Earth Sciences</b></p> <p>Discrimination of sediment provenance in the Yellow Sea: Secondary grain-size effect and REE proxy</p> <p>Hui-Soo Jung<sup>a</sup>, Dhongil Lim<sup>b,*</sup>, Do-Hyun Jeong<sup>c</sup>, Zhaokai Xu<sup>d</sup>, Tiegang Li<sup>e</sup></p>	<p><b>Journal of Asian Earth Sciences</b></p> <p>Holocene changes in detrital sediment supply to the eastern part of the central Yellow Sea and their forcing mechanisms</p> <p>Hui-Soo Jung<sup>a</sup>, Dhongil Lim<sup>b,*</sup>, Zhaokai Xu<sup>c</sup>, Jung-Hoon Kang<sup>d</sup></p>	<p><b>Estuarine, Coastal and Shelf Science</b></p> <p>Secondary grain-size effects on Li and Cs concentrations and appropriate normalization procedures for coastal sediments</p> <p>Hui-soo Jung<sup>a</sup>, Dhongil Lim<sup>b,*</sup>, Zhaokai Xu<sup>c</sup>, Kapsook Jeong<sup>d</sup></p>
<p><b>Palaeogeography, Palaeoclimatology, Palaeoecology</b></p> <p>Provenance discrimination of late deglacial and Holocene sediments in the southwest of Cheju Island, East China Sea</p> <p>Yanguang Doo<sup>a</sup>, Shouye Yang<sup>b,*</sup>, Dhongil Lim<sup>c</sup>, Hui-Soo Jung<sup>d</sup></p>	<p><b>Estuarine, Coastal and Shelf Science</b></p> <p>Quantitative comparison of grain-size effects in elemental concentration: A Korean coastal sediments case study</p> <p>Hui-Soo Jung<sup>a</sup>, Dhongil Lim<sup>b,*</sup>, Zhaokai Xu<sup>c</sup>, Jung-Hoon Kang<sup>d</sup></p>	<p><b>MARINE GEOLOGY</b></p> <p>Geochemical composition and provenance discrimination of coastal sediments around Cheju Island in the southeastern Yellow Sea</p> <p>S.Y. Yang<sup>a,b,*</sup>, D.I. Lim<sup>c</sup>, H.S. Jung<sup>d</sup>, R.C. Oh<sup>e</sup></p>
<p><b>Palaeogeography, Palaeoclimatology, Palaeoecology</b></p> <p>Clay-sized sediment provenance change in the northern Okinawa Trough since 22 kyr BP and its palaeoenvironmental implication</p> <p>Zhaokai Xu<sup>a,*</sup>, Tiegang Li<sup>b</sup>, Mengmeng Chang<sup>c</sup>, Shuang Wan<sup>d</sup>, Jinyong Choi<sup>e</sup>, Dhongil Lim<sup>f</sup></p>	<p><b>MARINE GEOLOGY</b></p> <p>Rare earth elements in bottom sediments of major rivers around the Yellow Sea: implications for sediment provenance</p> <p>Hui-Soo Jung<sup>a</sup>, Dhongil Lim<sup>b,*</sup>, Zhaokai Xu<sup>c</sup>, Kapsook Jeong<sup>d</sup>, Hui-soo Jung<sup>e</sup></p>	<p><b>Progress in Oceanography</b></p> <p>Paleoceanographic changes in the Ulleung Basin, East (Japan) Sea, during the last 20,000 years: Evidence from variations in element composition of core sediments</p> <p>Dhongi Lim<sup>a,*</sup>, Zhaokai Xu<sup>b</sup>, Jinyong Choi<sup>c</sup>, Seoyoung Kim<sup>d</sup>, Soza Kang<sup>e</sup>, Hui-soo Jung<sup>f</sup></p>
<p><b>Palaeogeography, Palaeoclimatology, Palaeoecology</b></p> <p>AGU PUBLICATIONS</p> <p><b>Paleoceanography</b></p> <p>RESEARCH ARTICLE</p> <p>New evidence for Kuroshio inflow and deepwater circulation in the Okinawa Trough, East China Sea: Sedimentary mercury variations over the last 20 kyr</p> <p>Dhongi Lim<sup>a,*</sup>, Hui-soo Jung<sup>b</sup>, Zhaokai Xu<sup>c</sup>, Kapsook Jeong<sup>d</sup>, and Hui-soo Jung<sup>e</sup></p>	<p><b>MARINE GEOLOGY</b></p> <p>Geochemical composition and provenance discrimination of coastal sediments around Cheju Island in the southeastern Yellow Sea</p> <p>S.Y. Yang<sup>a,b,*</sup>, D.I. Lim<sup>c</sup>, H.S. Jung<sup>d</sup>, R.C. Oh<sup>e</sup></p>	<p><b>Quaternary International</b></p> <p>Sediment provenance and paleoenvironmental change in the middle Okinawa Trough during the last 18.5 kyr: Clay mineral and geochemical evidence</p> <p>Zhaokai Xu<sup>a,*</sup>, Tiegang Li<sup>b</sup>, Peter D. Clark<sup>c</sup>, Dhongil Lim<sup>d</sup>, Qingyun Nan<sup>e</sup>, Shuang Wan<sup>f</sup>, Jinyong Choi<sup>g</sup>, Mengmeng Chang<sup>h</sup>, Hongbin Chen<sup>i</sup></p>

Raise up numerous problems in the previous studies (Yang and Lim et al., 2003, Lim et al., 2007)



**CYSM, SEYSM, SWCIM: source origin, transport pathway, and budget ?**



Ex.) SEYSM: Single or Mixed source of KR and CR ? / mixed ratio (contribution) ? / budget ? / transport pathway ?

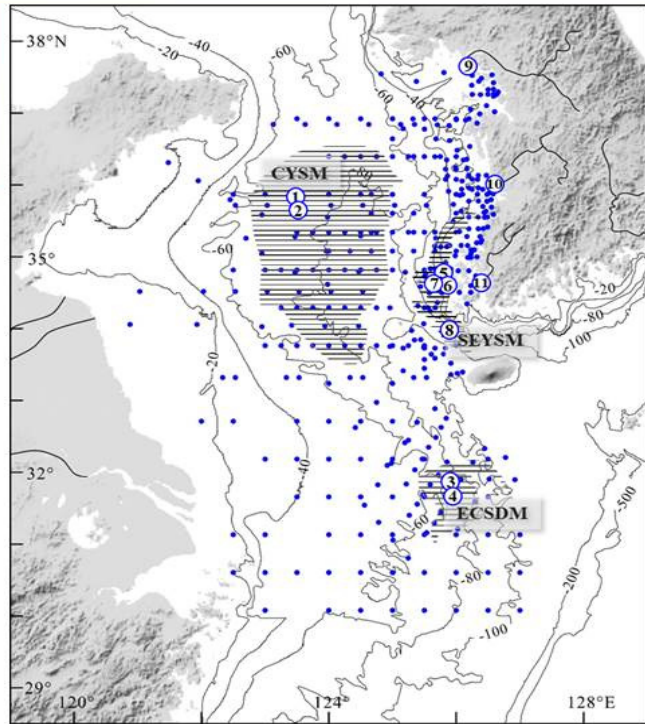


### 3. 연구 방법

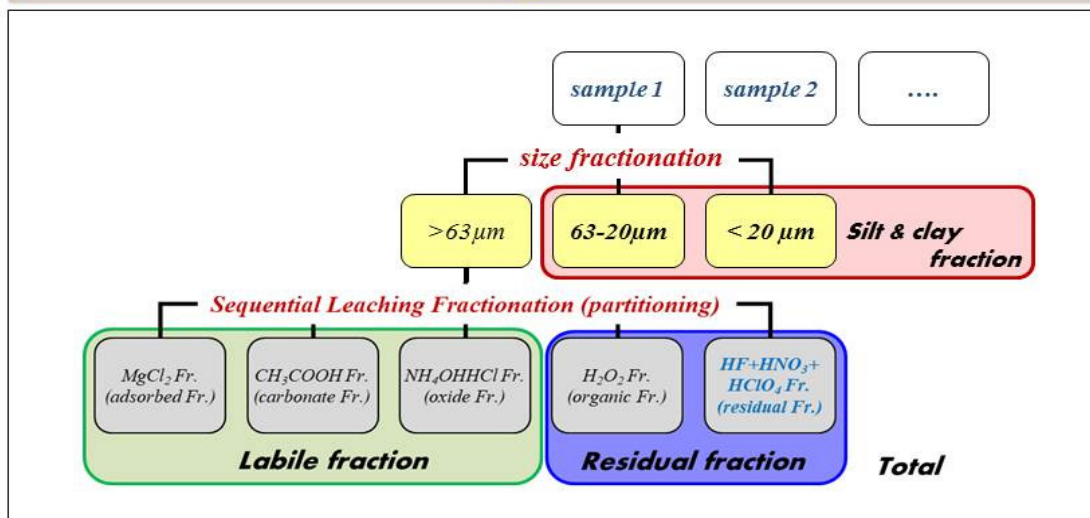
표층 퇴적물 시료: 420개

코어 퇴적물 시료: 11개 코어, 310개

주성분 및 희토류(REEs) 원소 분석



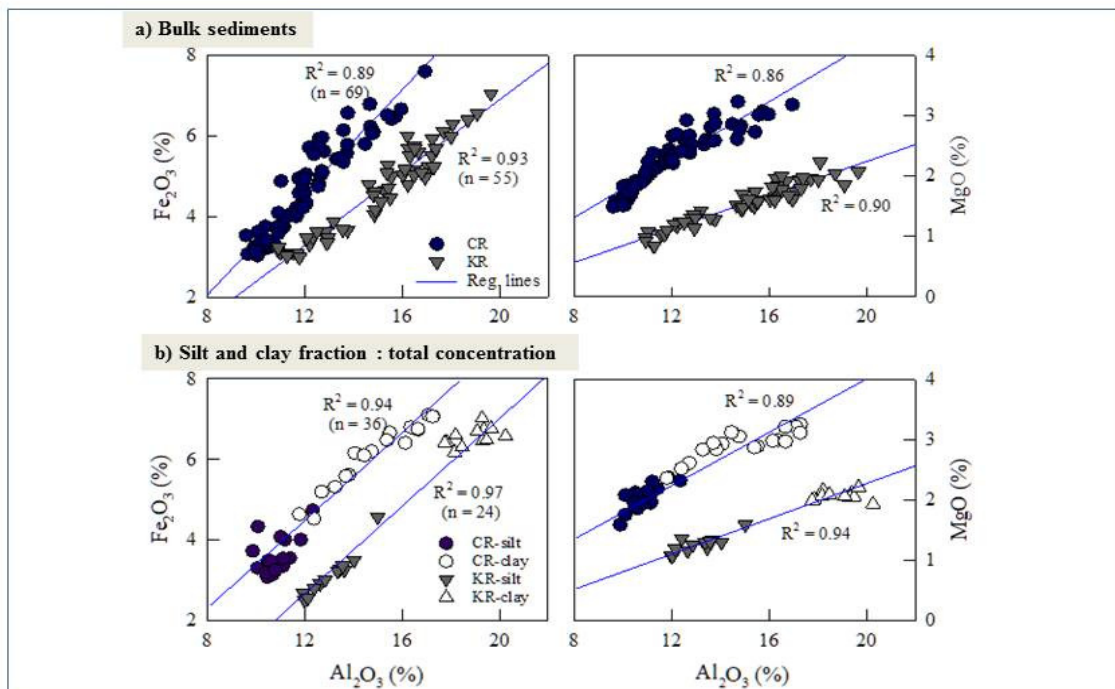
#### Normalization of grain size and chemical compositions: silt and clay particles / labile and residual fractions

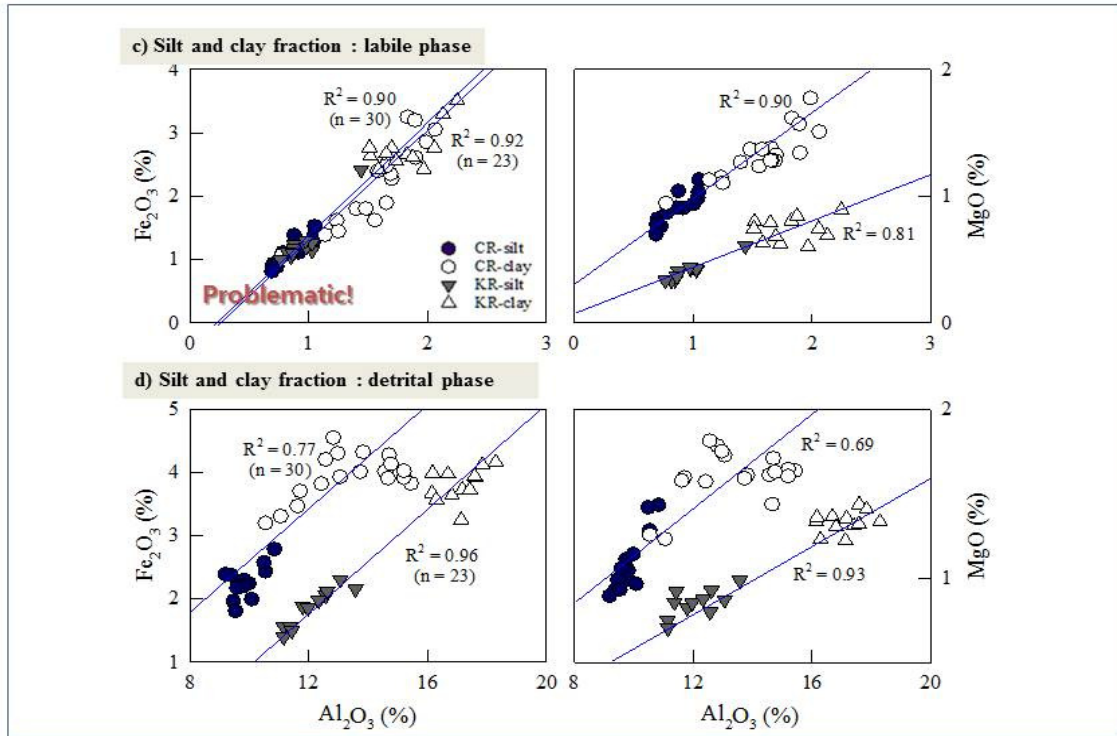


## 4. 연구 결과

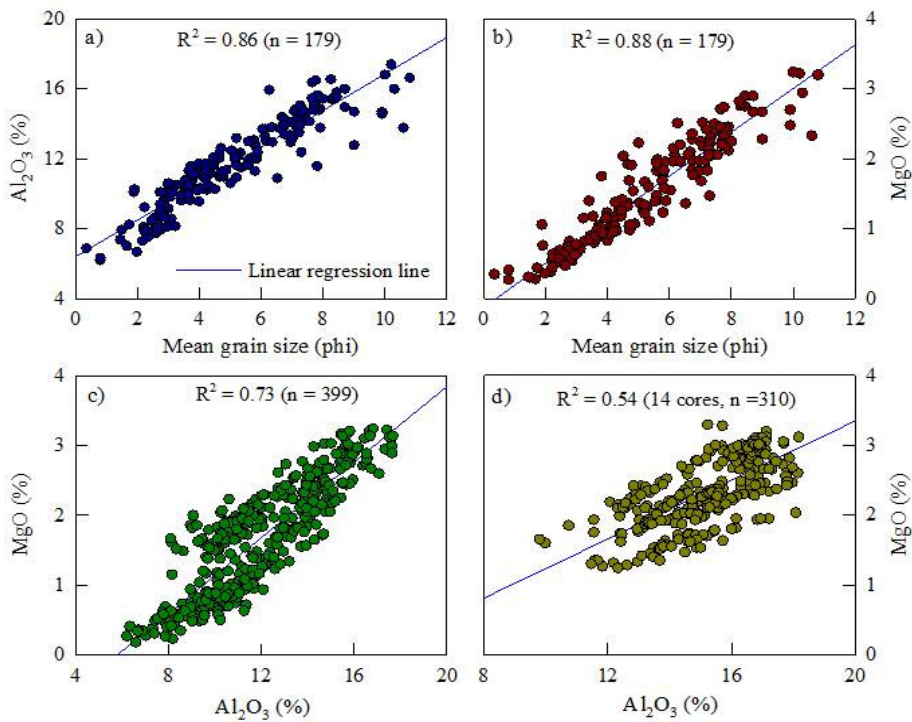
### 1. Al-Mg linear regression model

#### Provenance tracers for sediment discrimination





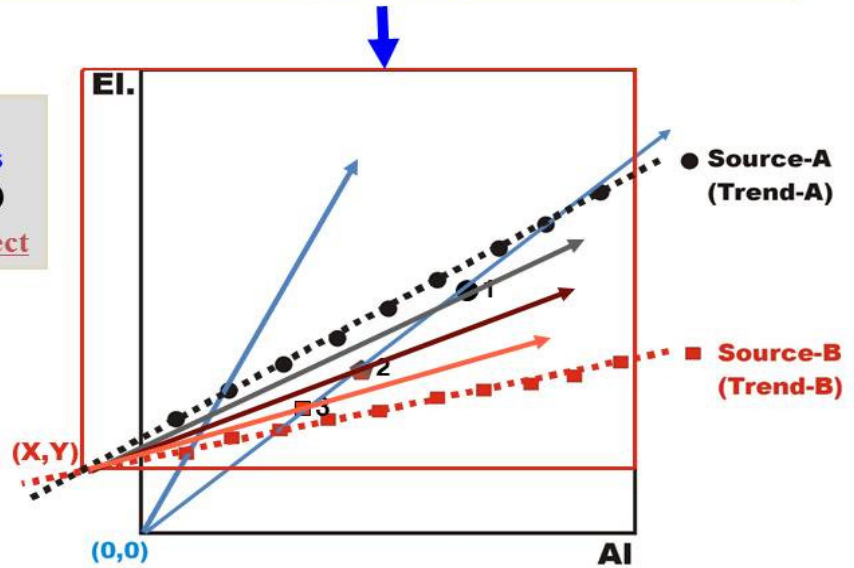
**Data analysis: 710 samples (this study)**



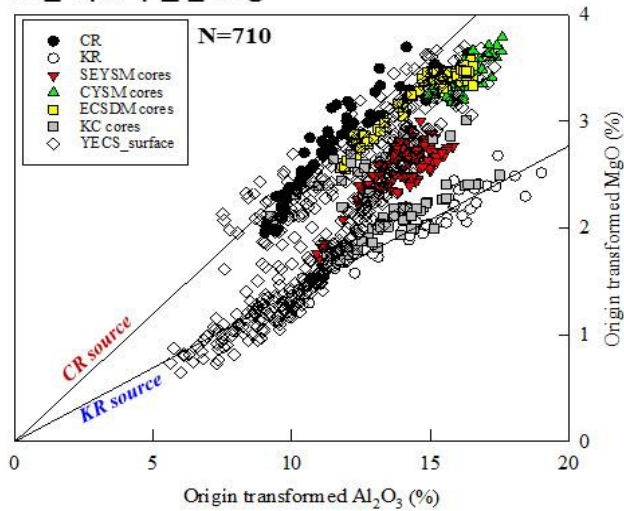
## A new approach for Quantification of S2S

In a restricted study area having two or three different sources, the general Al-normalized ratios (E/Al ratio) can give misleading information in determining the sediment provenance. For example,

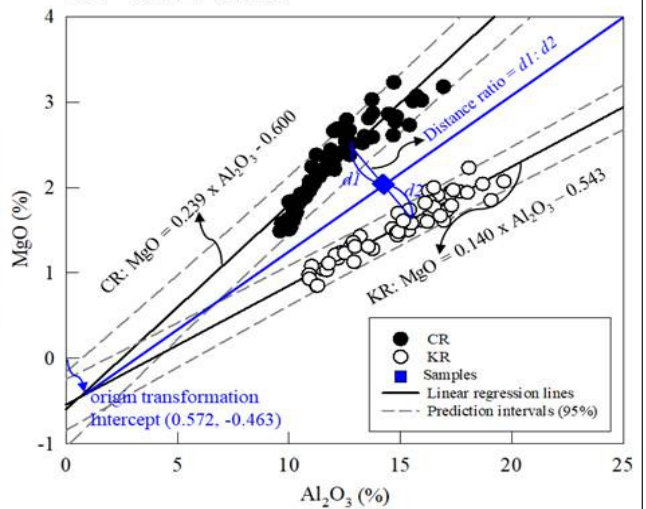
**Previous geochemical tracers : Element/Al ratios (Fe/Al, Mg/Al, V/Al ratios)**  
 → Sediment grain-size effect



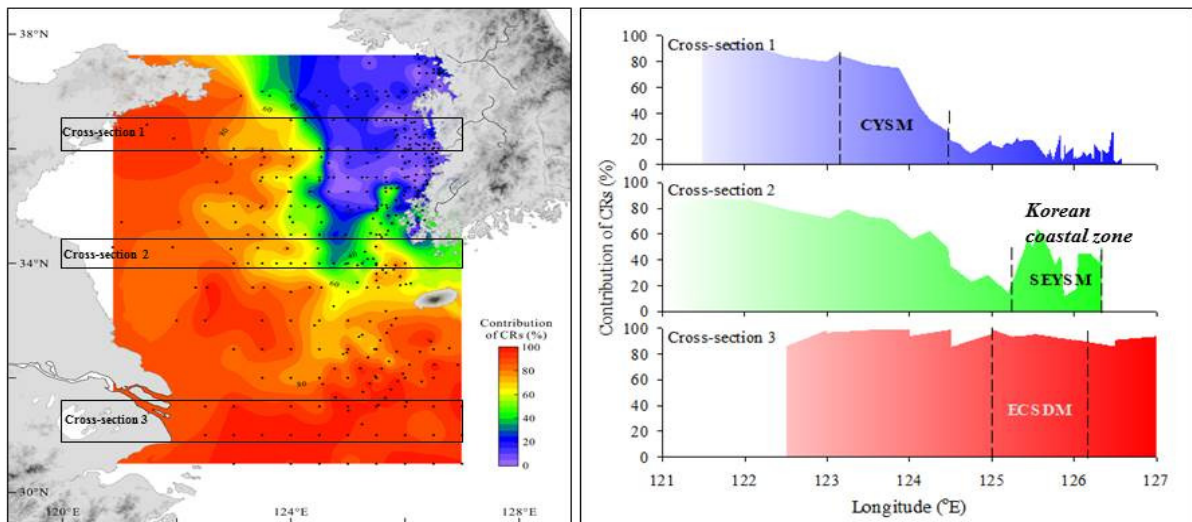
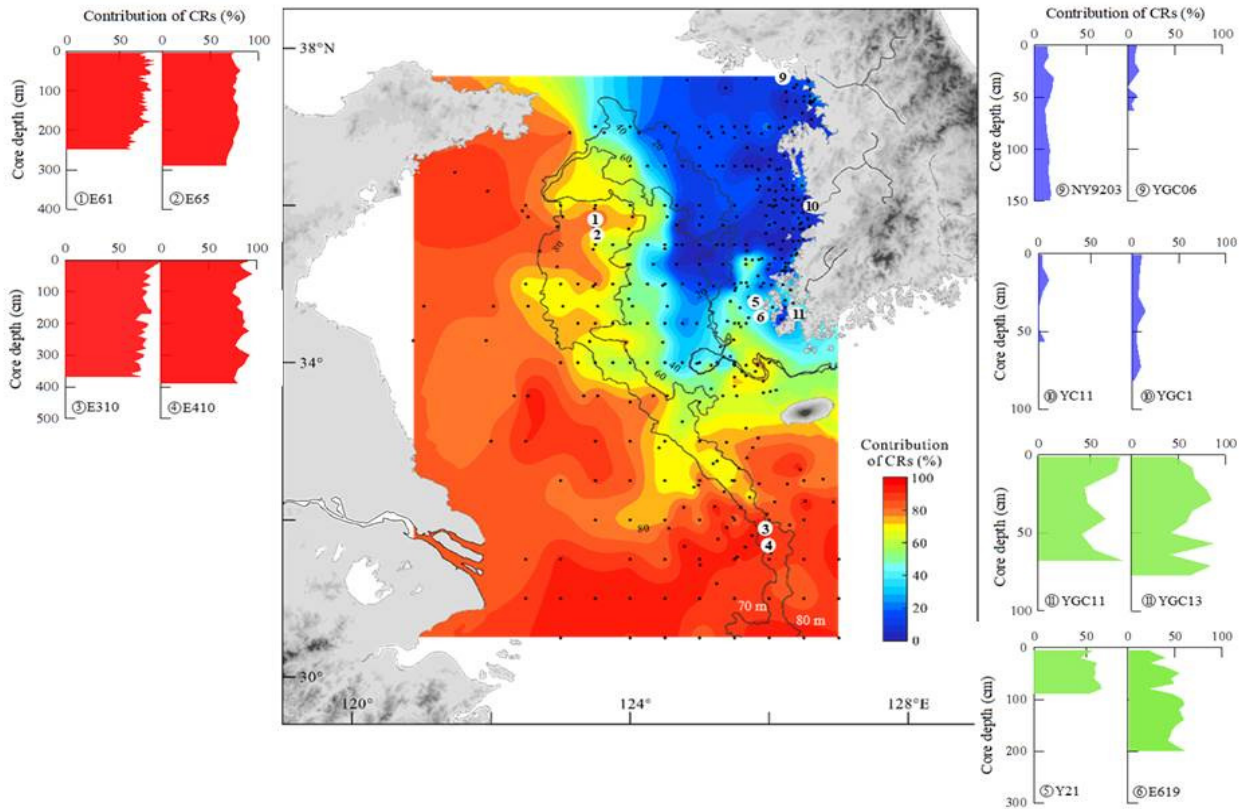
모든 자료의 원점 보정



모든 시료의 전량화

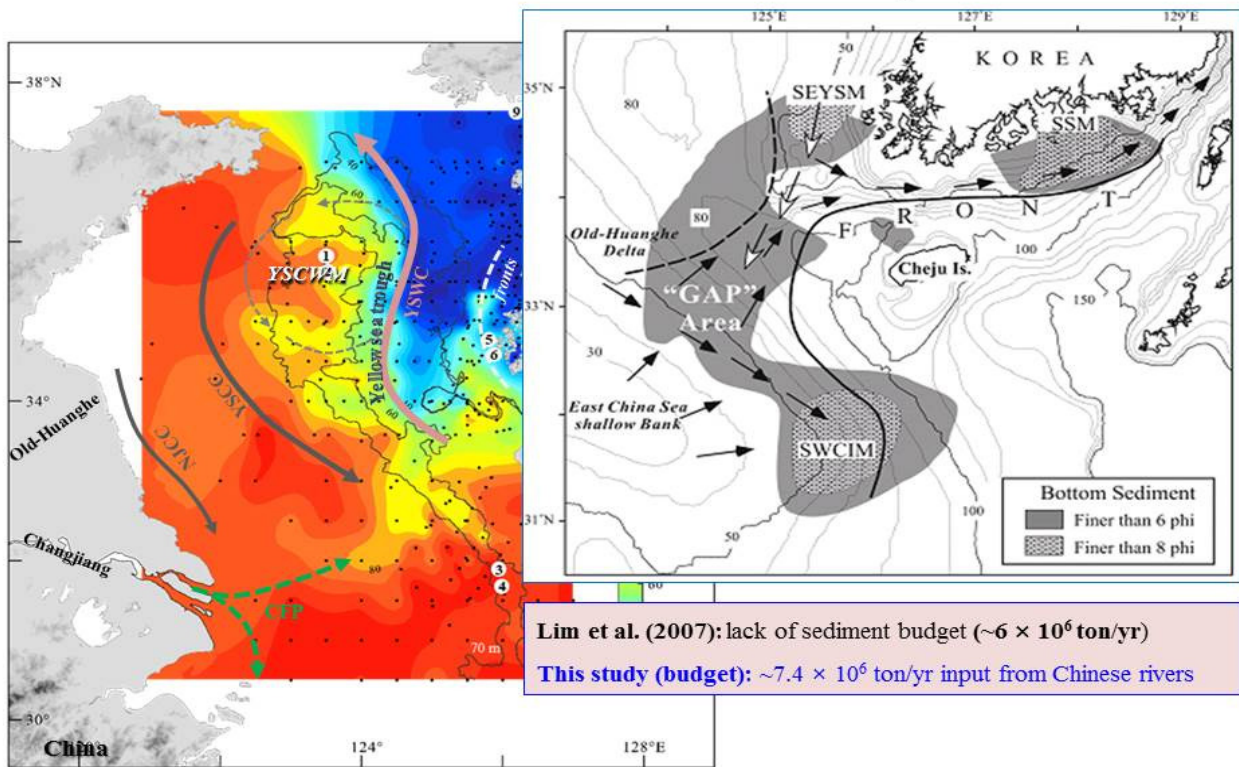


## Spatial distinction between KR and CR attributions

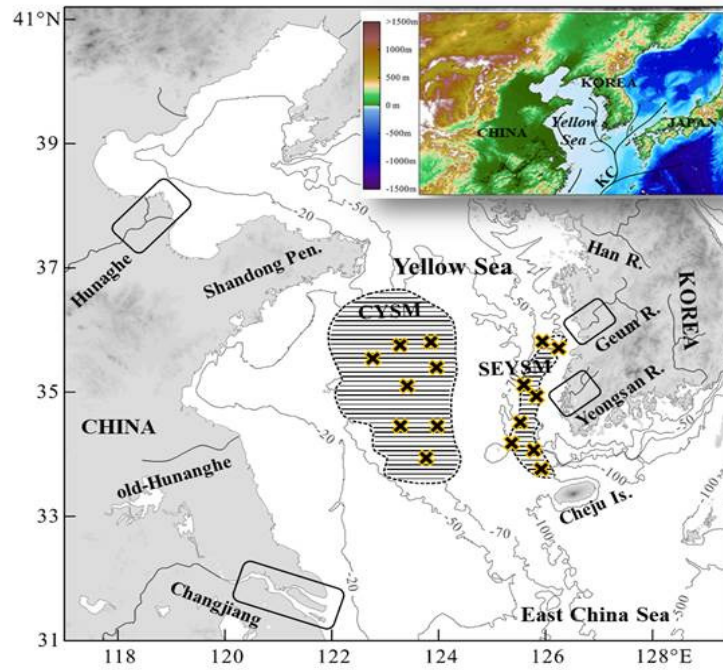




## SEYSM source and budget

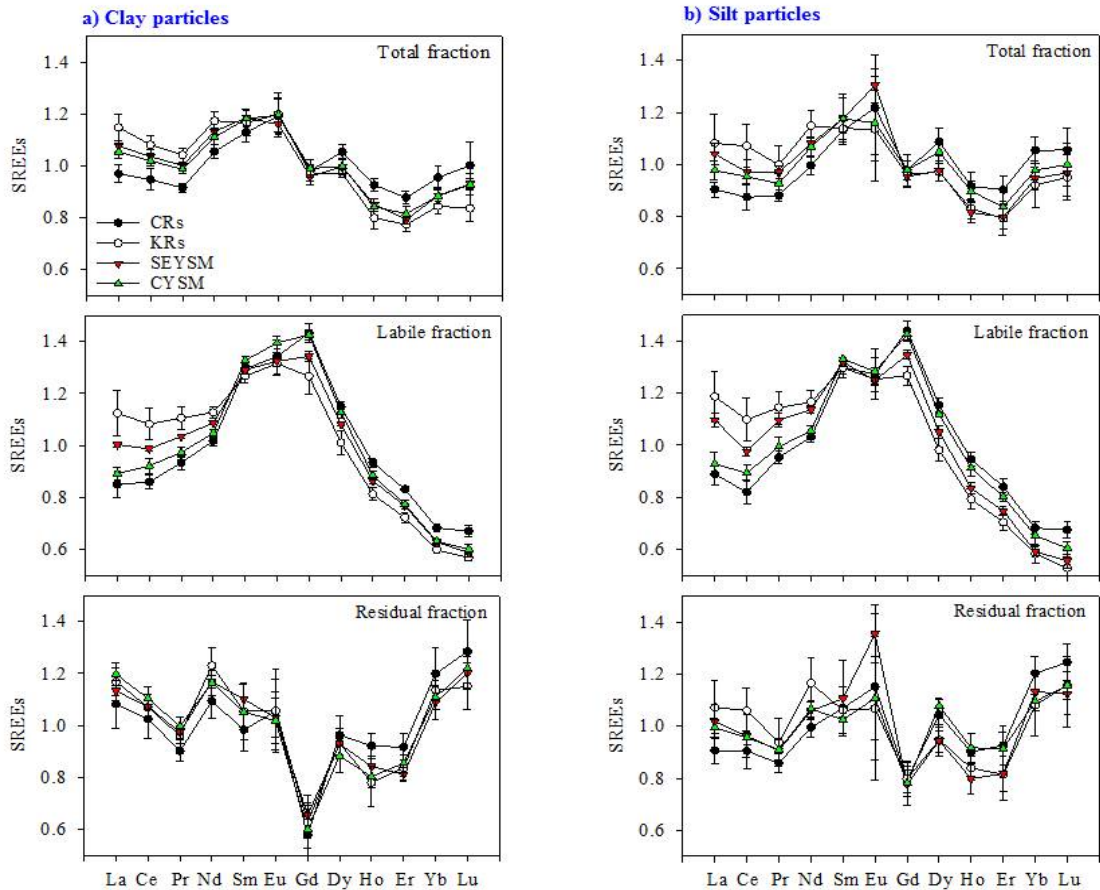


## 2) REE fractionation pattern model



Sample analysis: major mud deposits

REEs : Bulk sediments → silt and clay fraction → labile and residual fraction



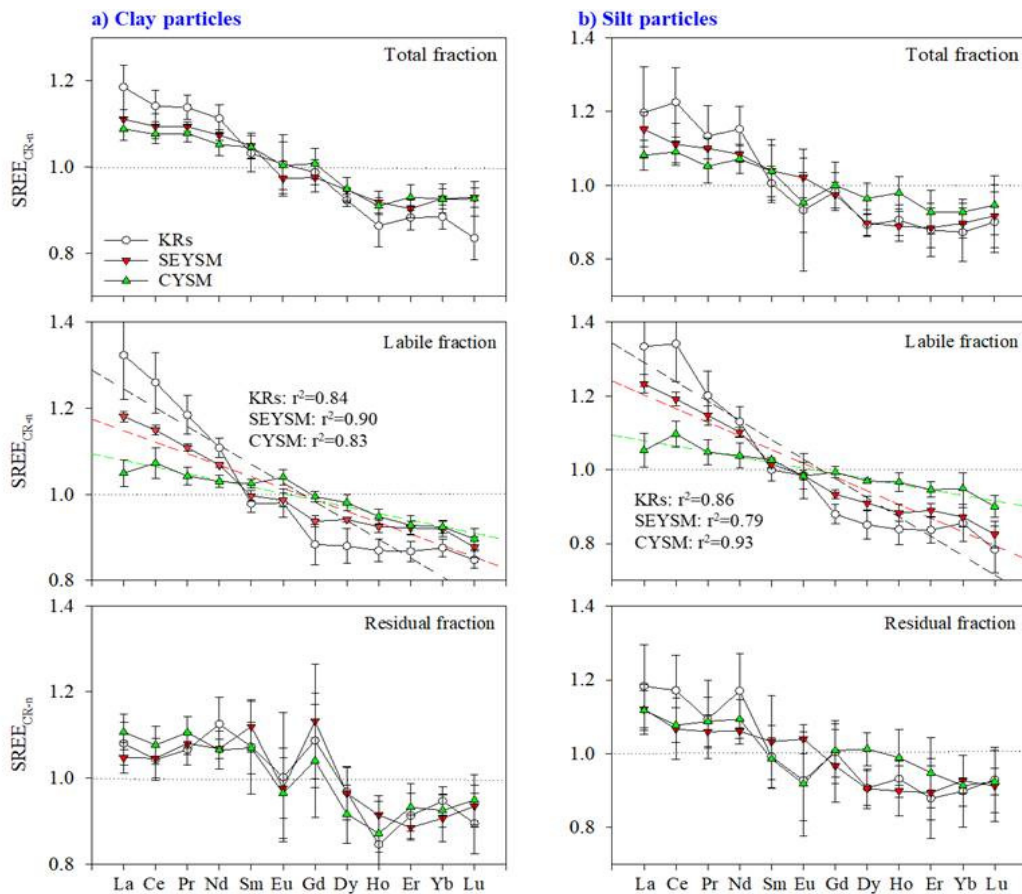
## This study

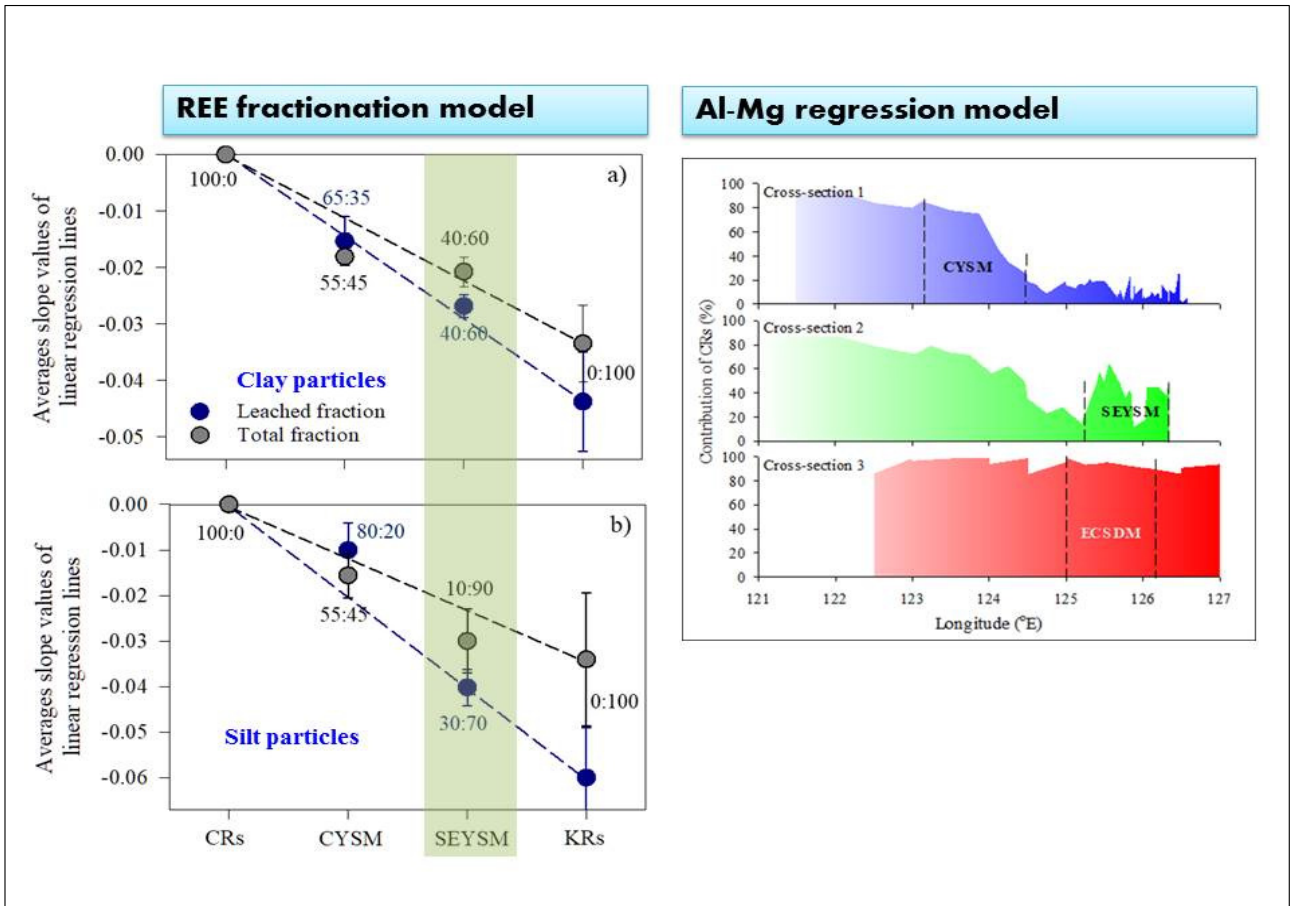
Standardization of REE<sub>UCC</sub> fractionation pattern

$$\sum_{i=La}^{Lu} \left( \frac{C_i}{(\sum_{j=La}^{Lu} C_j)/n} \right) = 12 \quad (\text{Eq. 1})$$

$i = La, Ce, Pr, Nd, Sm, Eu, Gd, Dy, Ho, Er, Yb, Lu, j = La, Ce, \dots Lu$

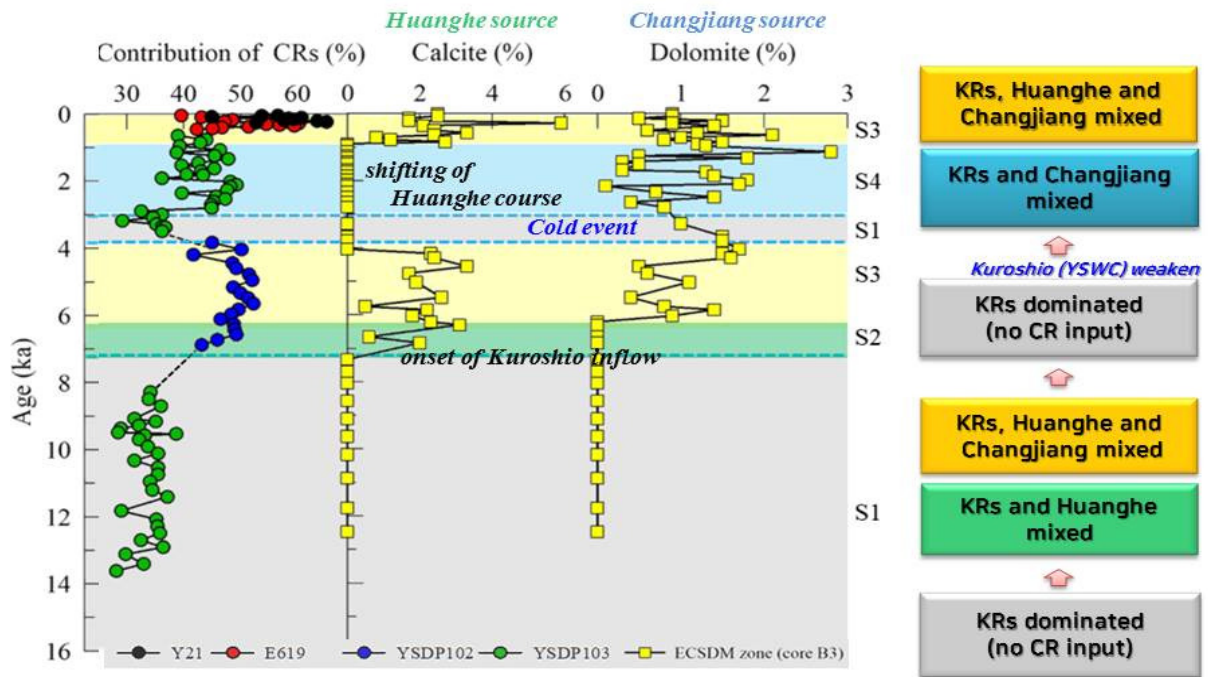
$C_{i(\text{or } j)}$ : UCC-normalized concentration ratio of REE (i or j);  $n = 12$  (number of i (or j))





### 3) 퇴적물 기원지의 시간적 변화와 원인

#### Holocene sediment source variations in SEYSM and SWCIM zones



## 5. 연구 결과 및 성과

- 1) 기존 시료 활용 및 분석: 황해-북동중국해 전 해역 표층 및 코어 퇴적물 시료 총 730개 시료, 지화학 성분 분석
- 2) 프록시 개발: Mg, Fe, (Ba), REEs
- 3) 정량화 모델 개발: Al-Mg regression model and REE fractionation model
- 4) 황해-동중국해 퇴적물의 S2S의 정량화 및 시공간적 변동 해석 및 해양과학적 자료 도출
- 5) 논문 성과: SCI 2편 / 국내 발표 1건

Marine Geology 430 (2020) 106345

Contents lists available at ScienceDirect

Marine Geology

journal homepage: [www.elsevier.com/locate/marge](http://www.elsevier.com/locate/marge)

Invited Research Article

Quantitative reconstruction of Holocene sediment source variations in the Yellow and northern East China Seas and their forcings

Dhongil Lim<sup>a,b</sup>, Jihun Kim<sup>a,b</sup>, Zhaokai Xu<sup>c</sup>, Hoisoo Jung<sup>d</sup>, Dong-Geun Yoo<sup>e</sup>, Mansik Choi<sup>f</sup>, So-Young Kim<sup>g</sup>

<sup>a</sup>South Sea Research Institute, Korea Institute of Ocean Science & Technology, Geopjeo 52201, Republic of Korea  
<sup>b</sup>POST School, University of Science & Technology, Daejeon 34124, Republic of Korea  
<sup>c</sup>CAS Key Laboratory of Marine Geology and Environment, Institute of Oceanology, Chinese Academy of Sciences, Qingdao 266071, China  
<sup>d</sup>Marine & Marine Debris, Korea Institute of Coastal and Mineral Resources, Daejeon 34132, Republic of Korea  
<sup>e</sup>Department of Oceanography, Chonnam National University, 99 Daehak-ro, Taehae-gu, Daejeon 34154, Republic of Korea  
<sup>f</sup>Division of Polar Ocean Science, Korea Polar Research Institute, Incheon 21900, Republic of Korea

CONTINENTAL SHELF RESEARCH

Editorial Manager

HOME • LOGOUT • HELP • REGISTER • UPDATE MY INFORMATION • JOURNAL DASHBOARD  
 MANUSCRIPTS • CONTACT US • SUBMIT A MANUSCRIPT • INSTRUCTIONS FOR AUTHORS • PRIVACY

Role: Author Username: ocaarim@kpost.ac.kr

Submissions Being Processed for Author Dhongil Lim

Page: 1 of 1 (1 total submissions) Display 10 results per page.

Action	Manuscript Number	Title	Initial Date Submitted	Status Date	Current Status
View Submission	CSR-0-20-0243	REE fractionation and quantification of sediment source in the Yellow Sea mud deposits, East Asian marginal sea	Sep 17, 2020	Oct 25, 2020	Under Review

Page: 1 of 1 (1 total submissions) Display 10 results per page.

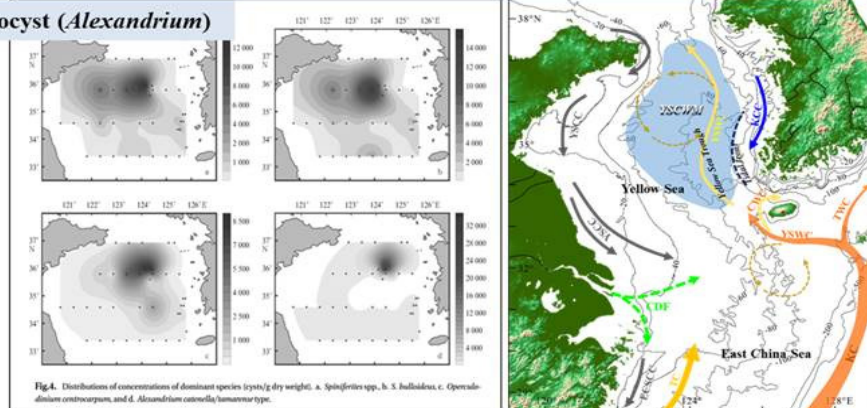
<< Author Main Menu

## 6. 연구 결과의 활용

- 한반도 주변 해양의 환경/생태계 특성 이해에 대한 해양지질학적 최신 정보 제공
- 국가적 해양환경/생태계 현안 문제 해결 및 대응 정책 수립을 위한 과학적 근거 자료 제공
- 황해-동중국해 관련 현안 사항 (해류 모델링, 전선역-냉수괴 환경/생태계 역할/연관성, 오염물질 정량화 등의 연구)들을 종합하는 체계적 연구 필요

### 황해 냉수괴/전선역의 해양학적(환경 및 생태계) 역할 규명

#### 예) Spatial distribution of dinocyst (*Alexandrium*)



## 주 의

1. 이 보고서는 한국해양과학기술원에서 수행한 주요사업의 연구결과 보고서입니다.
2. 이 보고서 내용을 발표할 때에는 반드시 한국해양과학기술원에서 수행한 주요사업의 연구결과임을 밝혀야 합니다.
3. 국가과학기술 기밀유지에 필요한 내용은 대외적으로 발표 또는 공개하여서는 안됩니다.